

AD 664574

①

LAMINAR HEAT TRANSFER TO A TWO-DIMENSIONAL BLUNT
FLAT NOSED BODY IN TRANSONIC AND SUPERSONIC FLOW.

by

Josef Rom and Arnan Seginer

Technion-Israel Institute of Technology
Department of Aeronautical Engineering,
Haifa, Israel

TAE REPORT No. 75



הטכניון - מכון טכנולוגי לישראל
הפקולטה להנדסה אווירונטית

DDC

FEB 7 1968

TECHNION - ISRAEL INSTITUTE OF TECHNOLOGY
DEPARTMENT OF AERONAUTICAL ENGINEERING

HAIFA, ISRAEL

E

This document has been approved
for public release and sale; its
distribution is unlimited.

Reproduced by the
CLEARINGHOUSE
for Federal Scientific & Technical
Information Springfield Va. 22151

UNCLASSIFIED

AD 664 574

LAMINAR HEAT TRANSFER TO A TWO-DIMENSIONAL
BLUNT FLAT NOSED BODY IN TRANSONIC AND SUPERSONIC
FLOW

Josef Rom, et al

Technion-Israel Institute of Technology
Haifa

September 1967

Processed for . . .

DEFENSE DOCUMENTATION CENTER
DEFENSE SUPPLY AGENCY



U. S. DEPARTMENT OF COMMERCE / NATIONAL BUREAU OF STANDARDS / INSTITUTE FOR APPLIED TECHNOLOGY

UNCLASSIFIED

F61052 67 C 0033

SR - 3

September 1967

SCIENTIFIC INTERIM REPORT No. 3

LAMINAR HEAT TRANSFER TO A TWO-DIMENSIONAL BLUNT
FLAT NOSED BODY IN TRANSONIC AND SUPERSONIC FLOW.

by

Josef Ron and Arnan Seginer
Technion- israel institute of Technology
Department of Aeronautical Engineering,
Haifa, Israel

TAE REPORT No. 75

The research reported in this document has been sponsored in part by the Aerospace Research Laboratories, under the Contract F61052 67 C 0033, through the European Office of Aerospace Research (OAR) United States Air Force. This research is part of the Separated Flow Research Program of the ARL, Thermomechanics Division.

This document has been approved for public release and sale; its distribution is unlimited.

ABSTRACT

Heat transfer rates are measured on a two-dimensional, blunt, flat nose and in the separated and reattaching flow regions of the separation bubble behind the leading edge corners in the high enthalpy laminar transonic and supersonic flow in the shock tube.

The measurements are carried out in a shock Mach number range from 2.5 to 10, and a corresponding flow Mach number from approximately 0.4 (the flow being choked) to 2.7. The Reynolds number, which is based on half of the nose height, varies from 8×10^2 to 3.3×10^4 and the local Reynolds number on the flat plate section, behind the leading edge corners, based on the distance from the stagnation point varies from 1×10^3 to 1.5×10^5 .

The results are correlated in terms of: (Nu/Pr) , $(q/\sqrt{P_1})$ and $(Nu/PrRe^{1/2})$ as functions of Mach and Reynolds numbers and stagnation to wall enthalpy ratios. The variations of local maximum and average heat transfer rates on the nose section and in the separation bubble region behind the corner are presented.

<u>TABLE OF CONTENTS</u>	<u>PAGE No.</u>
ABSTRACT	i
TABLE OF CONTENTS	ii
LIST OF FIGURES	iii
NOMENCLATURE	iv
I. INTRODUCTION	1 - 2
II. EXPERIMENTAL APPARATUS	3
A. The Shock Tube and its instrumentation	3
B. Heat Transfer Model	4 - 6
C. Flow Uniformity	6 - 7
III. HEAT TRANSFER RATE MEASUREMENTS	7 - 8
A. Heat Transfer Measurements Over the Leading Edge Separation Bubble	8 - 11
B. Flat Nose Heat Transfer Measurements	11 - 13
IV. DISCUSSION OF RESULTS	
1. Comparison Between Heat Transfer Distribution Over a Flat Nose and a Flat Base	13 - 15
2. Heat Transfer Distribution About the Leading Edge Separation Bubble	16 - 18
REFERENCES	19 - 20

LIST OF FIGURES

<u>Fig. No.</u>	
1	The 10" x 12" Hypersonic shock tube - shock tunnel
2	Blunt Flat Nosed Heat Transfer Model
3	Heat Transfer Gages Output
4	Establishment Time of Steady State Conditions
5(a - d)	Local Nusselt Number vs. Re_x on flat plate section
6(a - d)	Local Nusselt Number on Blunt Leading Edge vs. Re_h
7(a - d)	Heat Transfer Variation on Blunt Leading Edge
8(a - d)	Heat Transfer Rate Variation Behind Corner Separation
9(a, b)	$q/p_1^{1/2}$ vs. Shock Mach Number
10(a, b)	$Nu_x/PrRe_x^{1/2}$ vs. Shock Mach number.

NOMENCLATURE

h	- Half height of leading edge
M_2	- Flow Mach number behind initial shock wave in the shock tube
M_f	- Flow Mach number over model
M_s	- Shock Mach number
Nu_x	- Local Nusselt number on flat plate section, based on distance from stagnation point
Nu_h	- Local Nusselt number on leading edge based on half leading edge height
P_1	- Initial pressure in the shock tube low pressure section
Pr	- Prandtl number
q	- Local heat transfer rate
$q_{f.p.}$	- Flat plate heat transfer rate
$q_{s.p.}$	- Two dimensional stagnation point heat transfer rate
Re_x	- Reynolds number on flat plate section based on distance from stagnation point
Re_h	- Reynolds number based on half leading edge height
t	- Time
x	- Local length coordinate measured from stagnation point

INTRODUCTION

As part of the separated flows and near wake studies underway at the Department of Aeronautical Engineering of the Technion-Israel Institute of Technology, heat transfer rates were measured over the two dimensional blunt base of a wedge-flat plate in the shock tube [1]. The heat transfer rates variation across the base surface were found to be in the subsonic flow cases and in some supersonic flow experiments wavy with multiple peaks. Since the reversed flow in the base region (near the base's center) resembles to some degree stagnation point flow it was tried to compare these results with stagnation point heat transfer data. Two flow geometries were considered for comparison:

- (a) A two dimensional jet impinging on a vertical wall which may be similar to the central part of the recirculating wake impinging on the base
- (b) a blunt flat nose exposed to uniform flow.

However very little experimental information was found about such configurations in the range of parameters experienced in our shock tube experiments. Measurements of heat transfer from a free jet to a wall [2] were compared with the data of [1] and some qualitative agreement was found. Still it is felt that the base flow cannot be strictly analogous to the impinging jet case. Therefore it was decided to investigate the blunt flat nose configuration. This configuration was chosen because technically it was easy to obtain simply by turning the wedge-flat plate

base heat transfer model described in [1] with the base facing upstream, thus getting a blunt flat two dimensional nose as the leading edge of the model in the two dimensional flow of the shock tube.

The blunt flat nose heat transfer data is interesting in itself since all hyper velocity vehicles use blunted noses at their leading edges to reduce the intense heat transfer rates. As the maximum local heat transfer rate in most cases will still occur at the forward stagnation point or its vicinity, the heat transfer rates associated with this region are of considerable practical as well as theoretical interest and additional data is useful since the case of the flat two dimensional blunt nose has not yet been intensively investigated.

While the blunt nose heat transfer variations are investigated the heat transfer rates are also measured on the flat plate section of the model in the separating and reattaching flow behind the sharp corners of the leading edge. This information on the heat transfer rates in the leading edge separation bubble supplements previous studies of other separated flow configurations which were studied in this laboratory [1], [3] and [4].

Still the main object in the present work is not the blunt nose problem as such, but the comparison of the flat nose heat transfer rate data with that of the blunt base.

II. EXPERIMENTAL APPARATUS

A. The Shock Tube and Its Instrumentation

The heat transfer rate measurements are performed in the 75mm x 75 mm shock tube which is the straight channel section (unexpanded flow) of the Department's laboratory 10" x 12" hypersonic shock tunnel.

The shock tunnel (Fig. 1) consists of a cylindrical compression chamber 1.5 meter long, a square low pressure tube of 75mm x 75mm cross section 7 meters long and a double-expanded nozzle to a 10" x 12" hypersonic test section. The present measurements are performed in the test section at the end of the last section of the straight low pressure tube.

The low pressure section is evacuated to 1.5mm Hg. abs. using air as test gas. High pressure bottled air or hydrogen are used as driver gases in the compression chamber. A detailed description of the shock tube and the instrumentation is presented in [5].

The shock wave speed is determined by measuring the time of travel of the shock wave between two thin platinum film resistance thermometers mounted a known distance apart flush on the shock tube wall. The thin film gauges being under constant current react to the passage of the shock wave by a sudden jump in their output voltage which is fed through pulse amplifiers into a 10 Megacycle counter.

B. Heat Transfer Model

The model is a steel wedge-flat plate with a blunt edge (Fig. 2) spanning the shock tube test section. It is the same model that was used for blunt base heat transfer measurements [1] except that in the present experiments the blunt edge is turned upstream. The center part of the model is made of pyrex glass on which a number of thin platinum film gages are sputtered. Gages Nos. 1 to 6 and Nos. 11 to 13 are positioned on the top and bottom flat surfaces behind the leading edge corners and are used to measure the heat transfer rates in the leading edge bubble separating and reattaching flows. Four gages, Nos. 7 - 10 are positioned on the flat nose as shown in Fig. 2. The model chord is 41.09 mm and the leading edge height is $2h = 5.66\text{mm}$.

The positions of the nose gages centers from the nose center (stagnation point) and of the flat surface gages centers from the leading edge corners are given in Table No. 1. Given are also the non dimensional distances from the stagnation point- x/h .

TABLE I.

Position	Gage Nos.	distance from stagnation point X mm	distance from the corner mm	x/h
Leading Edge	7	-1.62	-	-0.572
	8	-0.08	-	-0.028
	9	1.26	-	0.444
	10	2.37	-	0.836
Flat Surfaces	3	11.83	9.00	4.176
	4	8.67	5.84	3.060
	5	6.02	3.19	2.125
	6	4.01	1.18	1.416
	11	3.65	0.82	1.289
	12	6.19	3.36	2.185
	13	9.06	6.23	3.198

The average width of the gages on the nose is approximately 0.8 mm.

The heat transfer gages are thin platinum film resistance thermometers sputtered on pyrex glass backing material. Every film is

calibrated and operated as described in [6]. The output of the gages is fed into an oscilloscope and into the analog computing network also described in [6] which turns the gage output into a step function directly proportional to the heat transfer rate. This step function is fed into the same oscilloscope through a 1 megacycle chopper thus displaying both signals simultaneously. The oscilloscope trace is then photographed. A typical example of the thin film gage output is shown in Fig. 3.

C. Flow Uniformity

Determination of flow conditions in the shock tube is inherently more difficult than in the low temperature continuous flow, and even if this is accomplished with acceptable accuracy, there are still two conditions that must be ascertained. The first is two-dimensionality and uniformity which are verified by the reproducibility of the results of consecutive shock tube runs. In the present work the reproducibility varies between $\pm 5\%$ and $\pm 10\%$ indicating uniform two-dimensional flow.

The second condition is that the heat transfer rate in the shock tube flow must reach steady conditions before the termination of the uniform hot flow. In the present work this condition is also fulfilled as indicated in Fig. 4. While the test times in this shock tube vary between $380\mu\text{sec}$ at $M_s = 2$ to about $90\mu\text{sec}$ at $M_s = 10$ the time of establishment of steady heat transfer conditions varies from $250\mu\text{sec}$ at $M_s = 2.5$ to $40\mu\text{sec}$ and $25\mu\text{sec}$ at $M_s = 10$ in the separated flow behind the leading edge

corner and on the nose near the corners respectively, and also from 70 μ sec at $M_s = 2.5$ to 25 μ sec at $M_s = 10$ in the vicinity of the nose center.

III. HEAT TRANSFER RATE MEASUREMENTS

Heat transfer rates are measured on the flat blunt leading edge of the model and in the separated flow and reattachment regions on the flat surface behind the sharp leading edge corners. The test range of flow conditions is obtained by varying the shock Mach number from 2.5 to 10. This is done, due to the shock tube's structural limitations, by changing the low pressure in the shock tube between 100 mm Hg. ab. to 1.5 mm Hg. ab. holding the high pressure driving gas to less than 600 psi. This procedure results in a simultaneous variation in flow Mach number, Reynolds number and stagnation to wall enthalpy ratio (the free stream stagnation temperature to wall temperature ratio varies in these tests from 5 to more than 50 when the shock Mach number is increased from 2.5 to 10.). This simultaneous variation of the main flow parameters complicates the interpretation of the data, the understanding of the individual effects and the importance of the various parameters. It is necessary to cross plot the results in order to obtain some indications as to the important parameters, while even then some results remain unexplained.

The free stream Reynolds number in these tests, Re_h , ranges from 8.4×10^2 to 3.3×10^4 , and the local Reynolds number on the flat surfaces of the model ranges from 1×10^3 to 1.6×10^5 . The flow Mach number behind the initial shock wave,

M_2 computed from the shock strength and real gas effects should vary from 1.00 to 2.64 but due to flow choking in the test section at $M_2 \approx 2$ (or $M_S \approx 5.65$, corresponding to all air driven and a few hydrogen driven runs) the real flow Mach number ranges from about 0.4 to 2.64. The lower limit of this range is not accurately known since the boundary layer displacement thickness on the shock tube walls can only be roughly evaluated. According to one dimensional flow theory and the test section and model dimensions choking should occur at $M_2 < 1.33$ or $M_S < 3.2$, but as will be shown in the next section, the present results clearly indicate choking up to $M_2 = 1.68$ ($M_S = 4.12$). Only for $M_2 > 2$ ($M_S > 5.65$) complete supersonic flow over the model is observed. This shows that the boundary layer on the walls has a strong effect on the flow blocking in the test section.

The heat transfer rates are determined from the output of both the thin film thermometers and the analog networks. The flow conditions are assumed to be the free stream conditions behind the initial shock wave. The use of the flow conditions behind the detached bow shock as reference conditions in the present test conditions did not result in any significant changes in the results, so that the free stream conditions were used in all regions of the flow. All the shock tube runs in the present work, even in the case of choked flow, are however characterized by a wall temperature that is considerably lower than the flow stagnation temperature and the present results correspond to highly cooled wall cases.

A. Heat Transfer Measurements Over the Leading Edge Separation Bubble

The heat transfer gages on the flat surfaces are positioned from about 1mm to 9 mm behind the leading edge corners. The local Nusselt number for each of the gages on

the flat surfaces is calculated from the measured heat transfer rate, the evaluated free stream conditions and the local length coordinate, x , measured from the stagnation point. The variation of the local Nusselt number with the local Reynolds number for these gages is shown in Figs. 5(a) to 5(d). Indicated in these figures for comparison is also the corresponding flat-plate, attached, laminar boundary layer heat transfer rate at the same free stream conditions given by

$$Nu_x = 0.33 Pr^{1/3} Re_x^{1/2}$$

The variation of the local heat transfer ratio $q/q_{f.p.}$ on the flat surfaces behind the leading edge sharp corner, where $q_{f.p.}$ is the corresponding attached plate value, is shown in Figs. 8(a) and 8(b) and the maximum and average relative heat transfer rates are given in Figs. 8(c) and 8(d) as functions of the Reynolds number and shock Mach number respectively.

Examination of the variation of the Nusselt number with the Reynolds number on the flat surfaces (Figs. 5(a) to 5(d)) in the separated and reattaching flow regions shows this variation to be linear (on log-log paper) and steeper than the flat plate attached flow variation, similar to the corresponding figures in [1], [3] and [4]. Figs. 5(a) to 5(c) display two levels of heat transfer at the same Reynolds number but at different flow Mach numbers. The lower Mach number line is higher and steeper. This seems to be due to flow choking so that the higher line indicates flow that is initially subsonic and separates at near sonic conditions. Comparison with Fig. 5 of Ref. [4] however discovers a contrast which

may indicate that separation of a uniform flow from a sharp leading edge step model and the separation of a flow while accelerating around a sharp corner are inherently different. In the step separation case we find that in the "dead water" region the variation of the Nusselt number is steeper than for attached flow and the flow is sensitive to disturbances such as choking, shock wave detachment or local transition effects whereas in the reattachment zone the line of Nu_x vs. Re_x parallels that of the attached flow and is insensitive to disturbances or Mach number variation. The present case of separation behind the sharp corner of the flat nose has the opposite characteristics. The data from gages Nos. 6 and 11 (Fig. 5d) that are closest to the corner and in fully separated flow falls on one line that parallels the attached flow line irrespectively of the free stream Mach number and flow condition (supersonic or choked) which can be explained by the fact that the flow in the vicinity of the corner is always near sonic. However the heat transfer rate variation further downstream (Fig. 5a-c) resembles the "dead water" data of [4].

In these shock tube runs due to technical limitations of the experimental system mentioned at the beginning of section III all of the free stream conditions are varied simultaneously and the effect of each main flow parameter cannot be experimentally investigated.

In an effort to separate these effects the data is replotted as $q/\sqrt{P_1}$ and $Nu_x/Pr Re_x^{1/2}$ as functions of the shock Mach number (Figs. 9a and 10a respectively)

In the case of laminar attached flow these parameters are independent of the Reynolds number and should indicate the effect of the flow Mach number and enthalpy ratio.

For the hydrogen driven runs (supersonic flow) the curves in Fig. 9(a) that correspond to the various gages have all the same form whereas when the flow is choked no common pattern is observed. Outstanding is the fact that in case of gages 11 and 6 that are closest to the corner the curves are continuous but for all other gages there is a sharp discontinuity between the parts corresponding to the choked and to the supersonic flows. This phenomenon will be discussed in section IV.

B Flat Nose Heat Transfer Measurements

The Nusselt number for the gages on the flat nose, is based on the nose height and free stream conditions. Its variation with the Reynolds number (also based on nose height) is shown in Figs. 6(a) to 6(d). Indicated in these figures for comparison is also the corresponding two dimensional, flat stagnation point heat transfer. It is based on the values given by Cohen and Reshotko [7] and Lees [8] for a two-dimensional cylindrical stagnation point modified by a factor of 0.665 to the flat nosed stagnation point [8] and [9]. This stagnation point value $q_{s.p.}$ is also used to compute the ratio of local nose to stagnation point heat transfer rate $q/q_{s.p.}$, the variation of which across the flat nose is shown in Figs. 7(a) and 7(b). Since the nose height is quite small (only 5.66 mm) there are only four heat transfer gages positioned on it and the width of the platinum strip (average width is 0.8 mm) is not negligible compared to the nose height. Thus the value of the heat transfer rate as measured by each gage is not a local value but an average over the strip width. By assuming a symmetrical heat transfer rate distribution and presenting each of the gages

readings also in its "mirror image" position (these reflected points are marked by flagged symbols for identification of the actually measured values) a plausible curve could be drawn through these readings with the curve passing through the gage strip width in such a manner that the area between curve and strip above the strip should equal that below the strip. In this way the measured value is an area average of the presented curve. This technique was also used in [1], but on second examination of the results there, it was found that in some cases, especially when the heat transfer rate distribution is wavy and the variation over the gage strip is large, totally different curves can be drawn without violating the equal areas rule. It was, therefore, decided not to place too much emphasis on the detailed local distribution and to indicate in the present paper only the average values (Figs. 7a and 7b). The relative width of each gage is indicated once in these figures and the average values are connected by straight lines in order to distinguish between the various shock tube runs.

Figs. 7(c) and 7(d) display the dependence of the local heat transfer rate peaks and the average heat transfer rate on the nose on the Reynolds and Shock Mach numbers respectively.

As in section IIIA the data for the flat nose is also replotted as $q/\sqrt{P_1}$ and $Nu_h/Pr(Re_h)^{1/2}$ vs. M_s in order to distinguish between the effects of the Reynolds and Mach numbers (Figs. 9b and 10b).

The curves of $q/\sqrt{P_1}$ vs. M_s in this case (Fig. 9b) are all continuous and

of about the same pattern contrary to the case of the separation bubble. Fig. 10b shows Gages Nos 8 and 9 to be the only gages that are nearly independent of the Mach number, apparently because these gages are very close to the nose center and the stagnation point flow is independent of the free flow Mach number.

The gages nearer the corner, however, show a combined effect of Reynolds and Mach numbers, similar to the case of the gages in the reattachment region on the flat surfaces behind the corners. These Reynolds and Mach numbers effects cannot be separated. In these regions the flow must be further investigated without the limitations on the variation of the flow conditions imposed by the present shock tube so that the individual effect and importance of the various flow parameters may be further determined.

IV. DISCUSSION OF RESULTS.

I. Comparison Between Heat Transfer Distributions Over a Flat Nose and a Flat Base

An interesting comparison is obtained between the relative heat transfer $q/q_{s,p}$, variation across the blunt base [1] and the present blunt nose (Figs. 7a-7b). On the blunt base two heat transfer variations were encountered. In the low M_s runs, when the flow is choked and the flow over the base is subsonic, the variation is very wavy with sharp slopes, with two peaks nearer the corner. These peaks are sometimes higher and in some cases are found to be lower than the center near stagnation point peak. In the high M_s runs, supersonic flow over the base, in addition to the wavy variation we find also a monotonic distribution with only one peak in the center at the rear stagnation region. These two types occur at

nearly the same free stream conditions which seems to indicate some instability in the near wake flow. It was assumed that this actual flow configuration is dependent on the existence or non existence of some disturbances such as transition effects or three dimensional (Ginoux) vortices. In the present flat nose case, the two different types of heat transfer variation which are observed are stable and repeatable Figs 7(a), 7(b). The subsonic and transonic flow cases, i.e., all of the air driven runs and some of the low shock Mach number hydrogen driven runs, have a W shaped heat transfer variation always with a peak at the center (forward stagnation point) and two much higher peaks near the corners. These corner peaks can be expected because of the flow acceleration around the corner as shown by Lees [8] and Kemp, Rose and Detra [10]. In the present work these heat transfer rate peaks are higher since the corners are sharp. The present measured variation is also more wavy than the theoretical curves in Refs. [8] and [10] but a similar behaviour can also be found in the experimental results of Ref. [9] and [10]. The value of the corner peak ($q/q_{s,p} = 1.65$) is almost constant in all subsonic runs as the flow there is near sonic in all these tests (also Figs. 7c, d). Interesting to note is that at gage No. 9 the heat transfer rate is rather constant ($q/q_{s,p} = 0.55$) even though the free stream conditions change, and the heat transfer indicated by the other gages varies considerably. The heat transfer rate at the forward stagnation point is somewhat lower than the values predicted by Cohen and Reshotko [7]. As the flow Mach number is increased from subsonic flow, (cases 1 to 5 in Fig 7a) to transonic flow (cases 6 and 7 in Fig 7a and cases

8 and 9 of the hydrogen driven runs) the heat transfer rate distribution has a monotonically changing W shape, then finally the supersonic pattern is observed (cases 10 to 13 of Fig. 7b). Here again a constant value of $q/q_{s.p.} = 1$, is measured at gage No. 9. This value is almost twice the subsonic flow value. Stagnation point heat transfer rates are again somewhat lower than the calculated values. The corner peak heat transfer rates grow as the flow Mach number is increased and the Reynolds number is reduced (Fig. 7c, d). It must be stated that although the two different types of heat transfer distribution are encountered in the present flat nose case for the subsonic and supersonic flow respectively, this case is inherently different from the blunt base heat transfer phenomena as observed in [1]. The heat transfer distributions on the flat blunt nose are stable and repeatable and change gradually from one into the other but in the case of the blunt base the distributions are not stable. Similar instability, but of a smaller magnitude, was also observed by Holden [9] on a blunt nose when he induced flow separation on a flat ended cylinder with a spike (Fig. 14 of [9]). He found that this also caused the total heat transfer to decrease to approximately one half of the unspiked value. This difference between spiked and unspiked (separated and attached) flow stability and total heat transfer rates resembles the differences between the separated unstable heat transfer rate distribution on the blunt base and the attached stable distribution on the flat blunt nosed model.

2. Heat Transfer Distribution About the Leading Edge Separation

Bubble

Due to the sharp corner at the blunt flat nose edge, the flow detaches there and a leading edge separation bubble is established just downstream of the corner. It has been indicated in Section IIIA that this kind of separation is different from the sharp leading edge step model separation [4]. Separation caused by the various types of steps are characterized by a closed cavity flow, whereas no such flow exists in the case of the leading edge or blunt nose corner separations. This difference in the types of flow separation is discussed and explained by Tani, Tsuchi and Komoda [1].

In the case of a leading edge separation the development of the flow may follow two possibilities:

- a) The flow may remain separated without reattaching. This is observed in the case of low Reynolds number laminar separation.
 - b) A separation bubble is established immediately behind the corner and the flow then reattaches further downstream.
- Tani [1,2] summarizes a number of results for subsonic leading edge separation bubbles. He shows that reattachment occurs when the Reynolds number, based on the boundary layer displacement thickness at the separation point, is greater than

500 In this case transition occurs in the flow over the bubble and it reattaches turbulently.

In the present work the heat transfer distribution over the flat surface just beyond the leading edge corner is shown in Figs. 8(a) and 8(b) for the subsonic and supersonic cases respectively. The very low values of heat transfer ($q/q_{\infty} = 0.9$) just beyond the corner indicate that the flow is separated there in all the runs. Further downstream the heat transfer rate increases and the maximum measured values of q/q_{∞} vary between 0.26 to 1.9 for subsonic flow case and 0.27 to 0.75 for supersonic flow, where the higher values are obtained at higher Reynolds numbers (Fig. 8(c)). It can not be firmly concluded from these distributions if the flow is fully reattached within the gaged section of the model. The variation of Fig. 9(a) may indicate some cases where no reattachment occurs, where the reattachment is not complete. The heat transfer variation of gages Nos. 6 and are continuous. These gages are nearest to the corner and are always within the separated flow region. On gages further away, there is a break in the heat transfer rate curve when the flow changes from subsonic to supersonic. This jump may indicate that in the high Reynolds number near sonic separation (low M_s data in Fig. 9a) the flow reattaches very close to the corner and the "short bubble" separation pattern [12] is established. While in the supersonic low Reynolds number case (high M_s data Fig. 9a) reattachment either does not occur or is more gradual as for the "long bubble" case [12].

The flow over the flat blunt nose is always subsonic in the present tests due to the normal shock ahead of the body, the flow downstream of the corner accelerates very rapidly to supersonic velocity in the high Mach number tests or to high subsonic and transonic velocities for the choked flow tests. Also the extent of the separation bubble is quite affected by the highly cooled walls experienced in the present tests. So that the comparison of the results from these tests with those of the low speed adiabatic results of References [11] and [12] can be only qualitative.

REFERENCES

1. Rom, J. and Seginer, A., "Laminar Heat Transfer to a Two-Dimensional Blunt Base from the High-Enthalpy Flow in the Shock Tube" Proc. IX Israel Ann. Conf. Aviation and Astronautics, Feb. 1967, Israel J. Tech. Vol. 5, No. 1-2, pp. 90-98, 1967. Also TAE Report No. 59, October 1966.
2. Gardon, R. and Akfirat, J. C., "The Role of Turbulence in Determining the Heat-Transfer Characteristics of Impinging Jets" Inst. J. Heat Mass Transfer, 8, 1261-1272, 1965.
3. Rom, J. and Seginer, A., "Laminar Heat Transfer to a Two-Dimensional Backward Facing Step from the High-Enthalpy Supersonic Flow in the Shock Tube" AIAA J., 2, 251-255, 1964.
4. Rom, J. and Seginer, A., "Laminar and Transitional Heat Transfer in the Two-Dimensional Separated Flow Behind a Sharp Protruding Leading Edge", Technion TAE Report No. 71, July 1967.
5. Rom, J. and Seginer, A., "Measurement of Laminar Heat Transfer Rates over a Two-Dimensional Backward Facing Step in a Shock Tube" Technion TAE Report No. 25, Feb. 1963.
6. Seginer, A., Cohen, A. and Rom, J., "Calibration of Thin Film Resistance Thermometers for Heat Flux Measurements in the Shock Tube. Proc. VII Israel Ann. Conf. Aviation and Astronautics, Feb. 1965. Israel J. Tech. Vol. 3, No. 1, 25-30, 1965.

REFERENCES (CONT'D)

- 7 Reshotko, E. and Cohen, C.B., " Heat Transfer at the Forward Stagnation Point of Blunt Bodies" NACA Tech. Note 3513, July 1955.
- 8 Lees, L. " Laminar Heat Transfer Over Blunt-Nosed Bodies at Hypersonic Flight Speeds" Jet Propulsion Vol. 26, 4, pp 259-269, April 1956.
- 9 Holden, M.S., " Preliminary Investigations on Heat Transfer Rates in Regions of Separated Flow" Imperial College of Science and Technology, Report No. 114, Sept. 1962.
- 10 Kemp, N.H., Rose, P.H. and Detra, R.W., " Laminar Heat Transfer Around Blunt Bodies in Dissociated Air" Jour. Aero/Space Sci. 26, 7, pp. 421-430, July 1959.
11. Tani, I., Iuchi, M. and Komoda, H., " Experimental Investigation of Flow Separation Associated with a Step or a Groove" Aero. Res. Inst. University of Tokyo, Rep. No. 364, Vol. 27, No. 4, Apr. 1961.
12. Tani, I., " Critical Survey of Published Theories on the Mechanism of Leading Edge Stall" Aero. Res. Inst. University of Tokyo, Report. No. 367, Vol. 27, No. 7, June 1961.

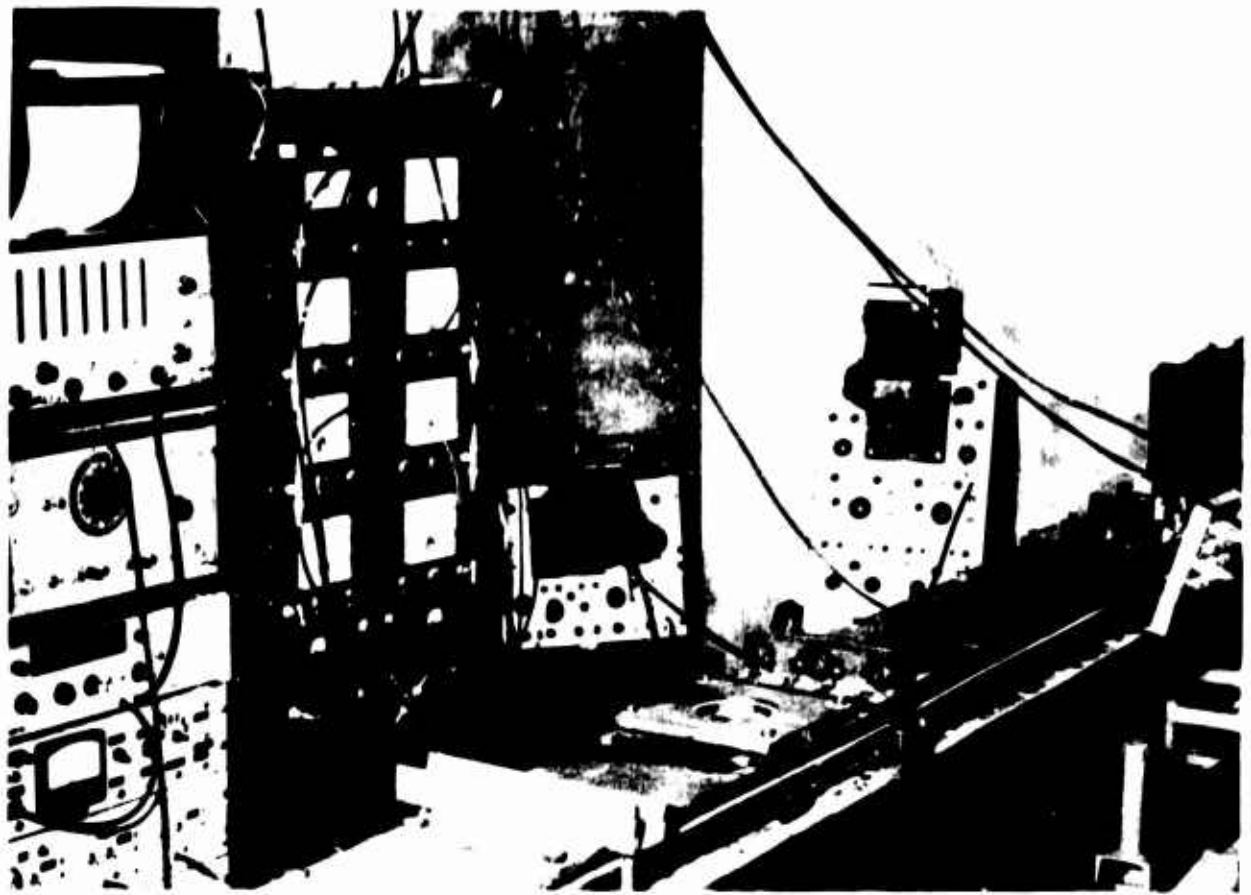


FIG. 1 - The 10" x 12" Hypersonic Shock Tube - Shock Tunnel

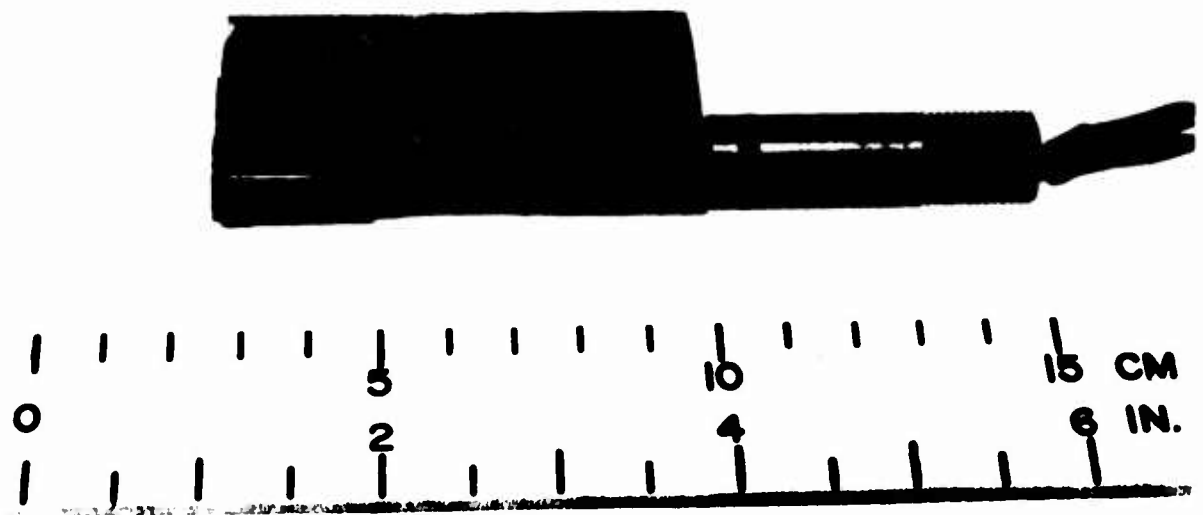
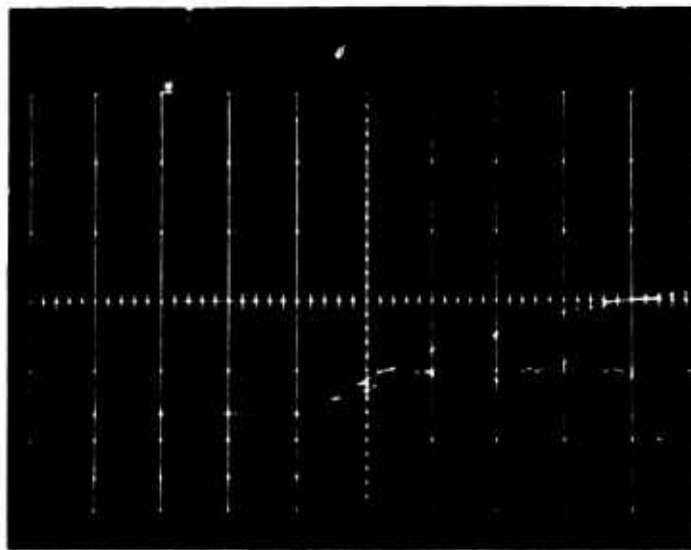


Fig. 2. - Blunt Flat Nosed Heat Transfer Model



3a) gage No. 9
 parabola - 50 mV/div. step - 500 mV/div.



3b) gage No. 7 }
 gage No. 10 } parabola - 50 mV/div.



3c) gage No. 5 parabola - 10 mV/div. step - 100 mV/div
 gage No. 6 parabola - 5 mV/div. step - 20 mV/div.

Fig. 3. - Heat Transfer Gages Output

$M_1 = 0.88$ $M_2 = 2.63$ $Re/cm = 9.46 \times 10^3$ Sweep = 20 μ sec/div

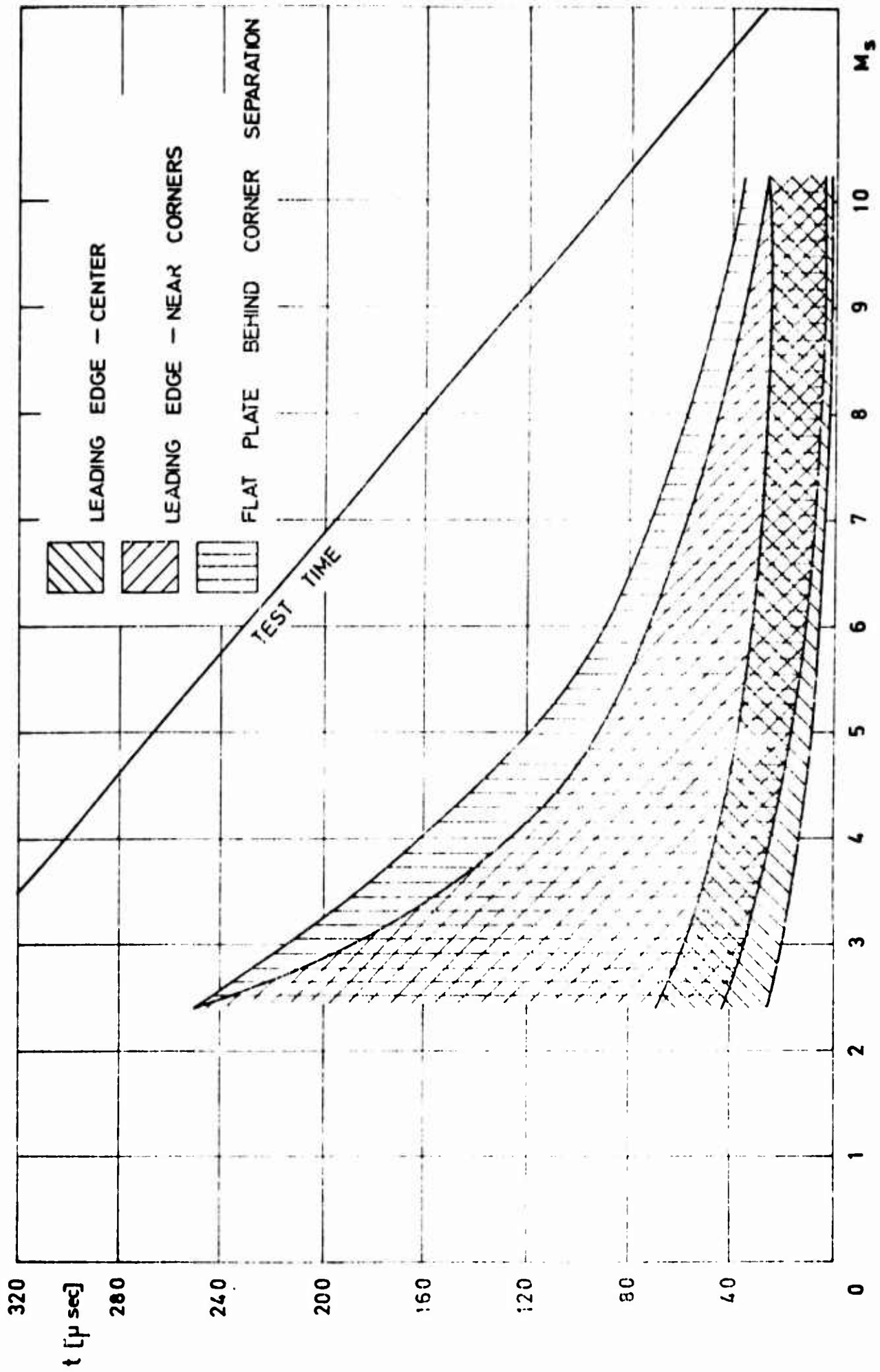


FIG. 4 ESTABLISHMENT TIME OF STEADY STATE CONDITIONS

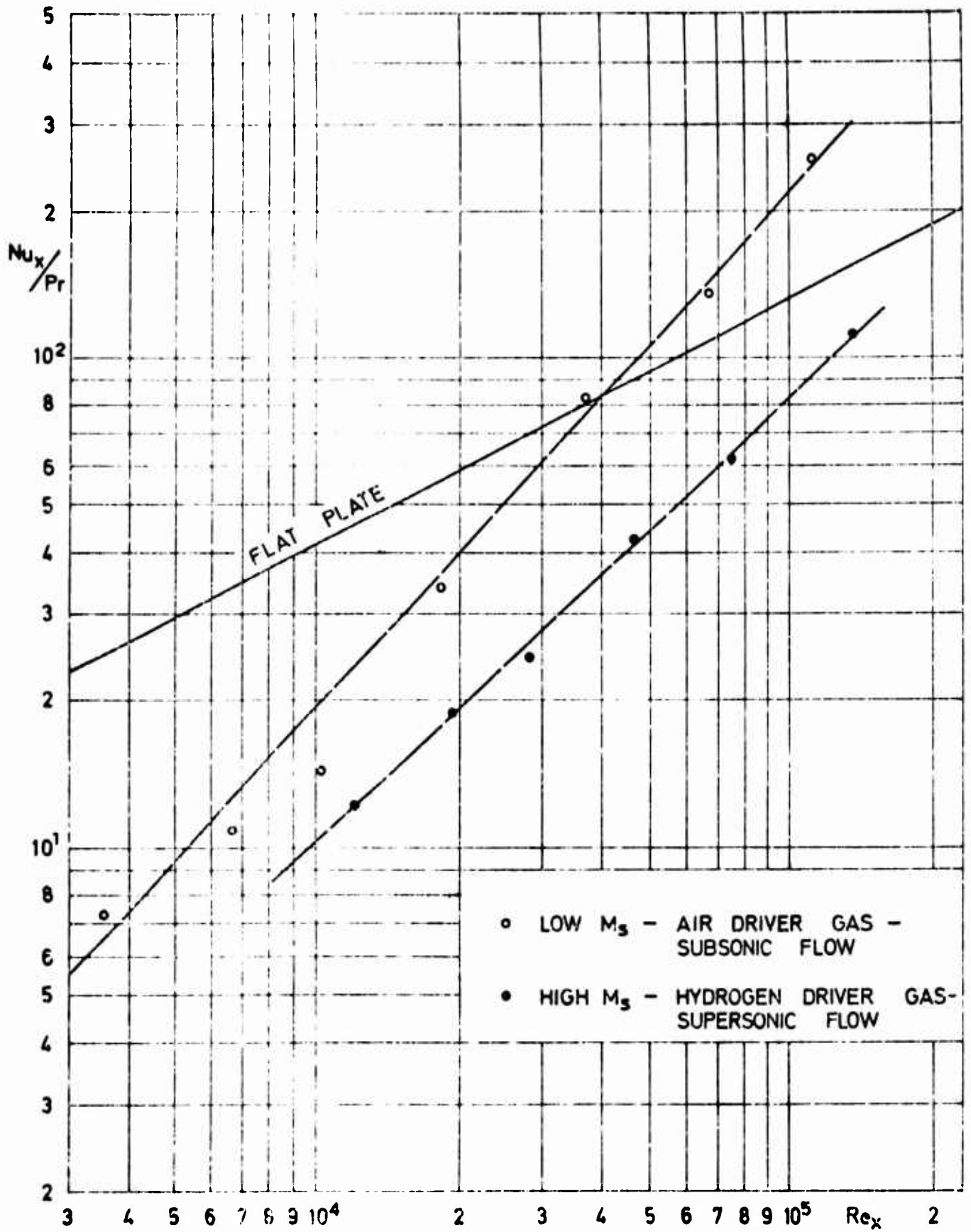


FIG. 5 LOCAL NUSSELT NUMBER VS. Re_x ON FLAT PLATE SECTION

a) GAGE NO. 3 AT $x/h = 4.176$

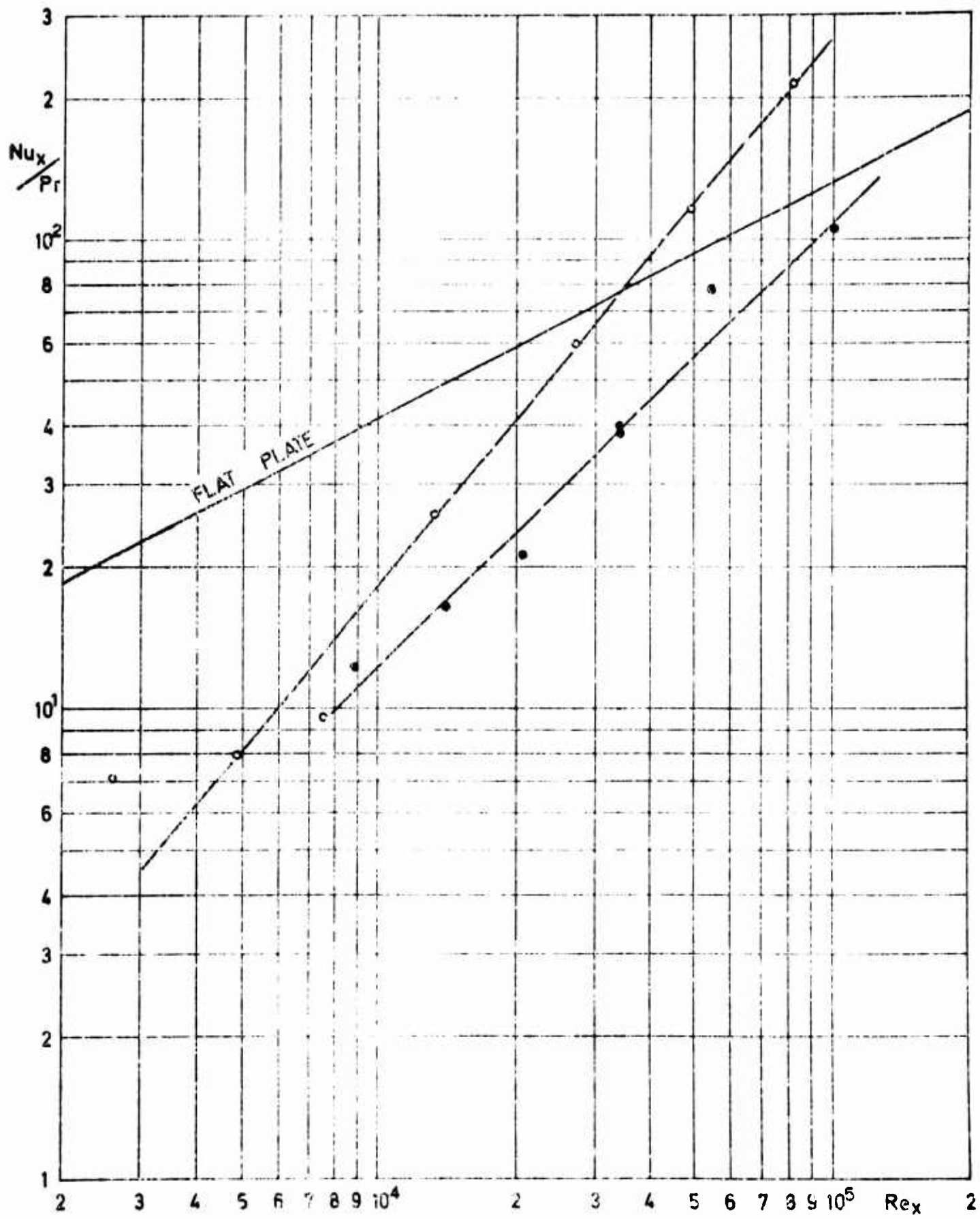


FIG. 5 (CONT.)

b) GAGE NO. 4 AT $x/h = 3.06$

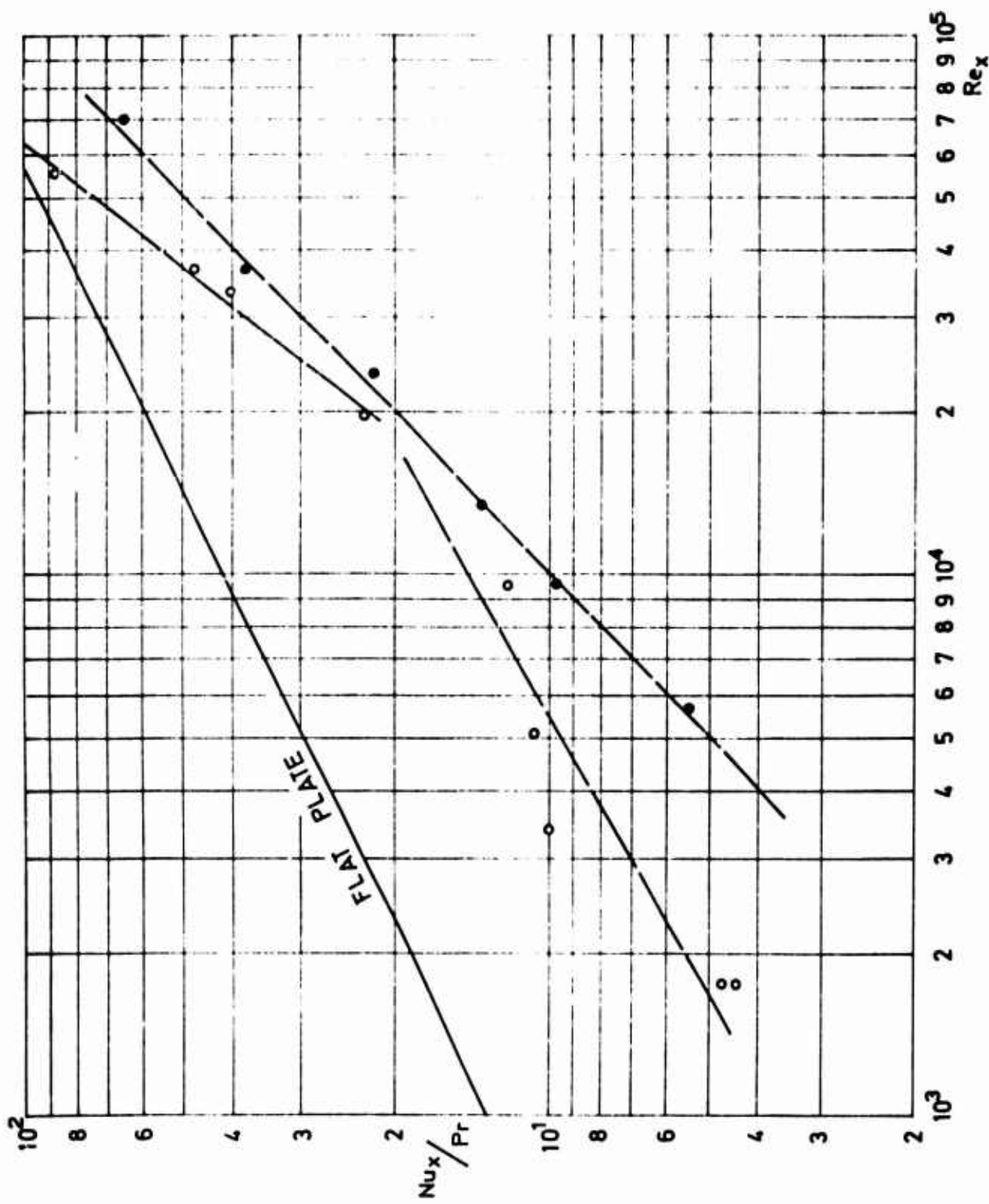


FIG. 5 (CONT.) c) GAGE NO. 5 AT $x/h = 2.125$

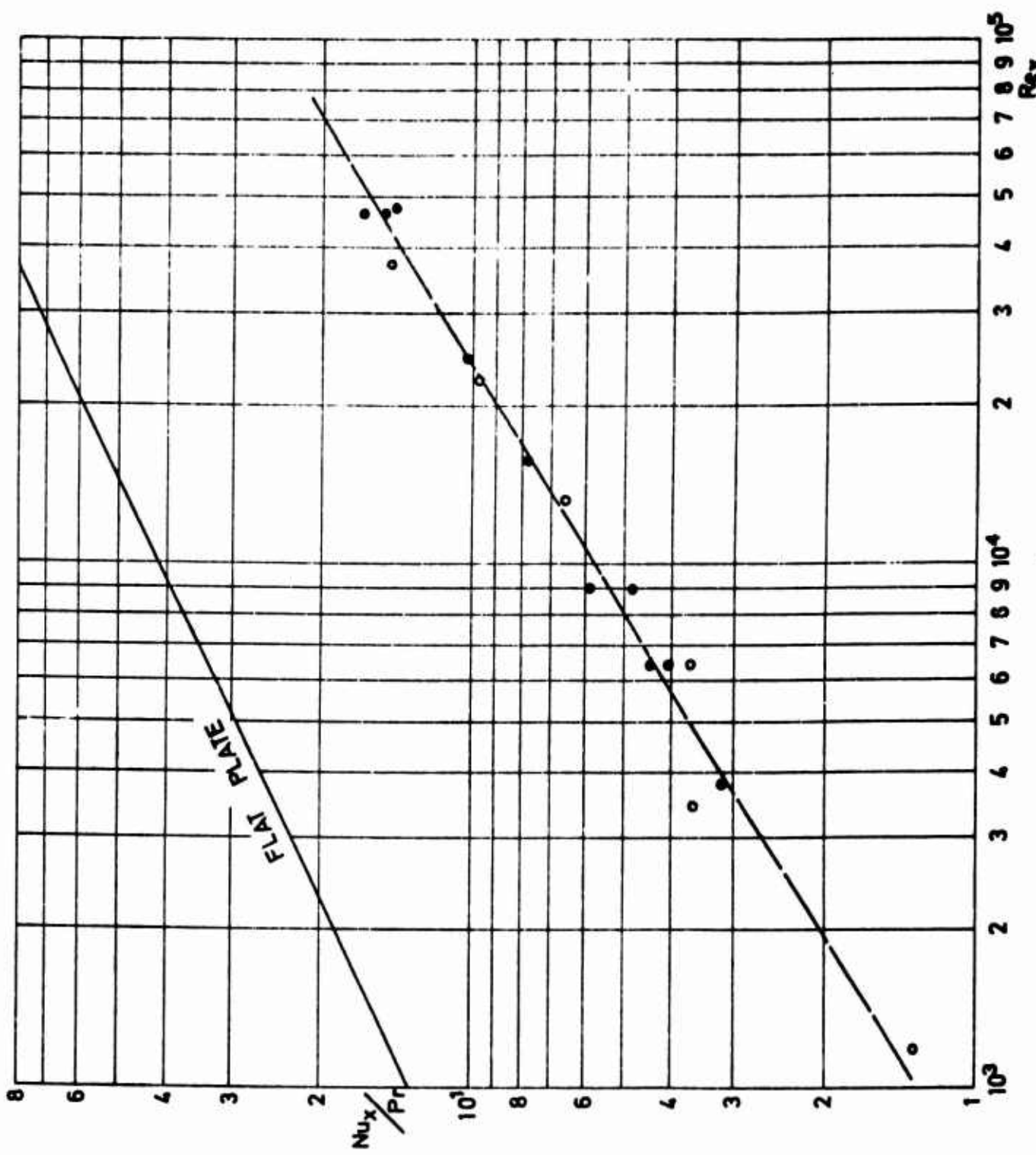


FIG. 5 (CONCL'D) d) GAGE NO. 6 AT $x/h = 1.016$

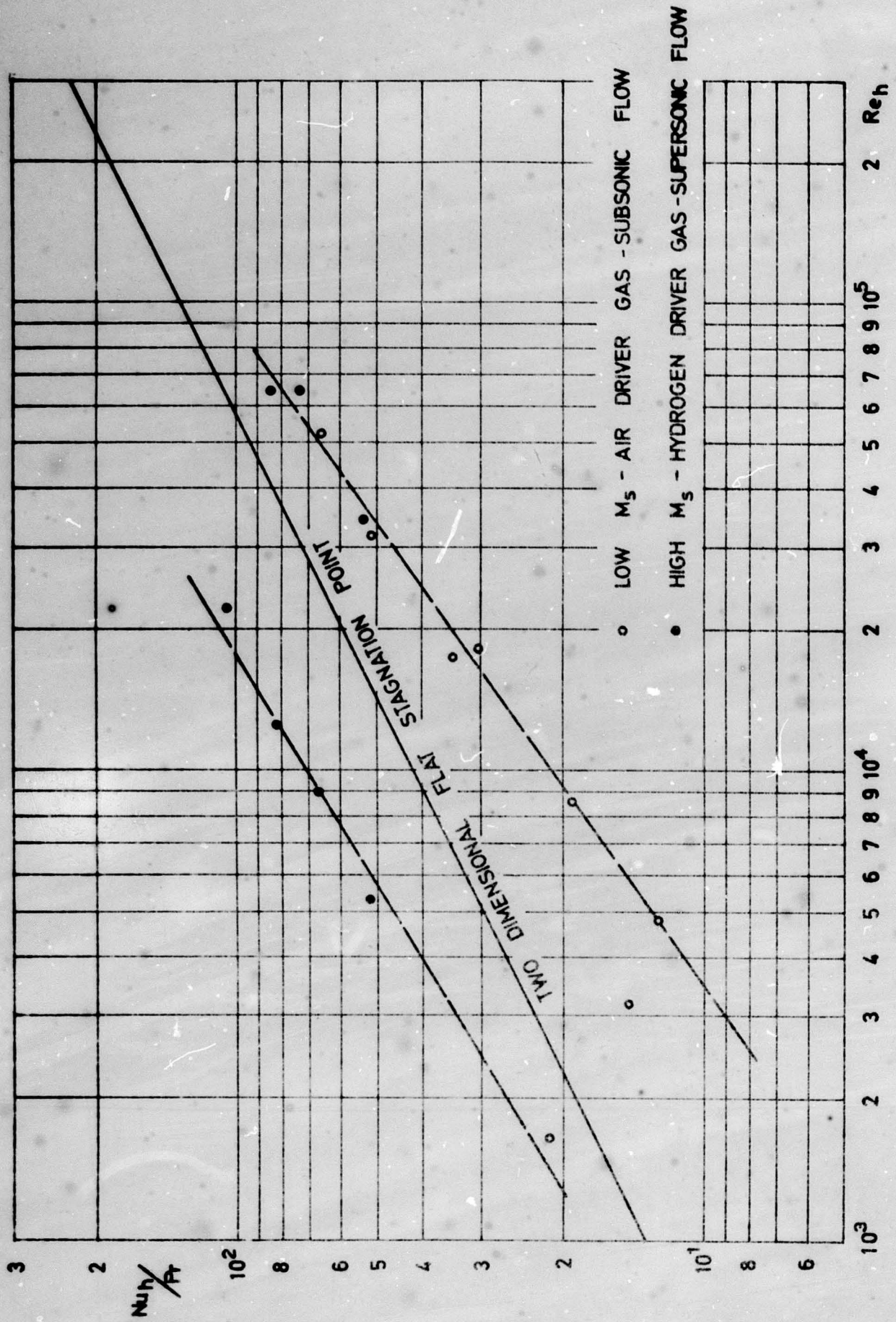


FIG. 6 LOCAL NUSSLETT NUMBER ON BLUNT LEADING EDGE VS. Re_h

a) GAGE NO. 7 AT $x/h = -0.572$

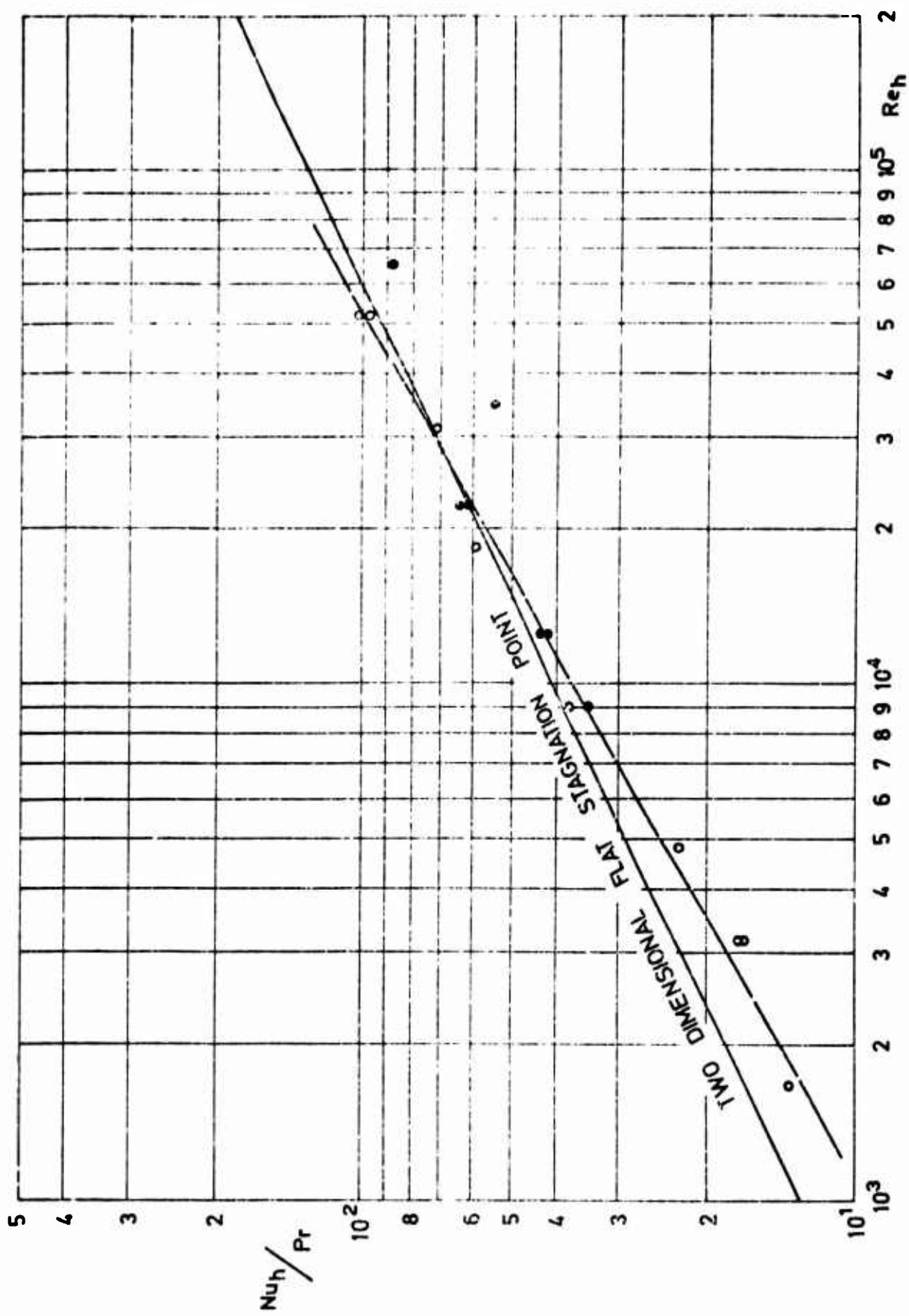


FIG. 6 (CONT.) b) GAGE NO. 8 - STAGNATION REGION

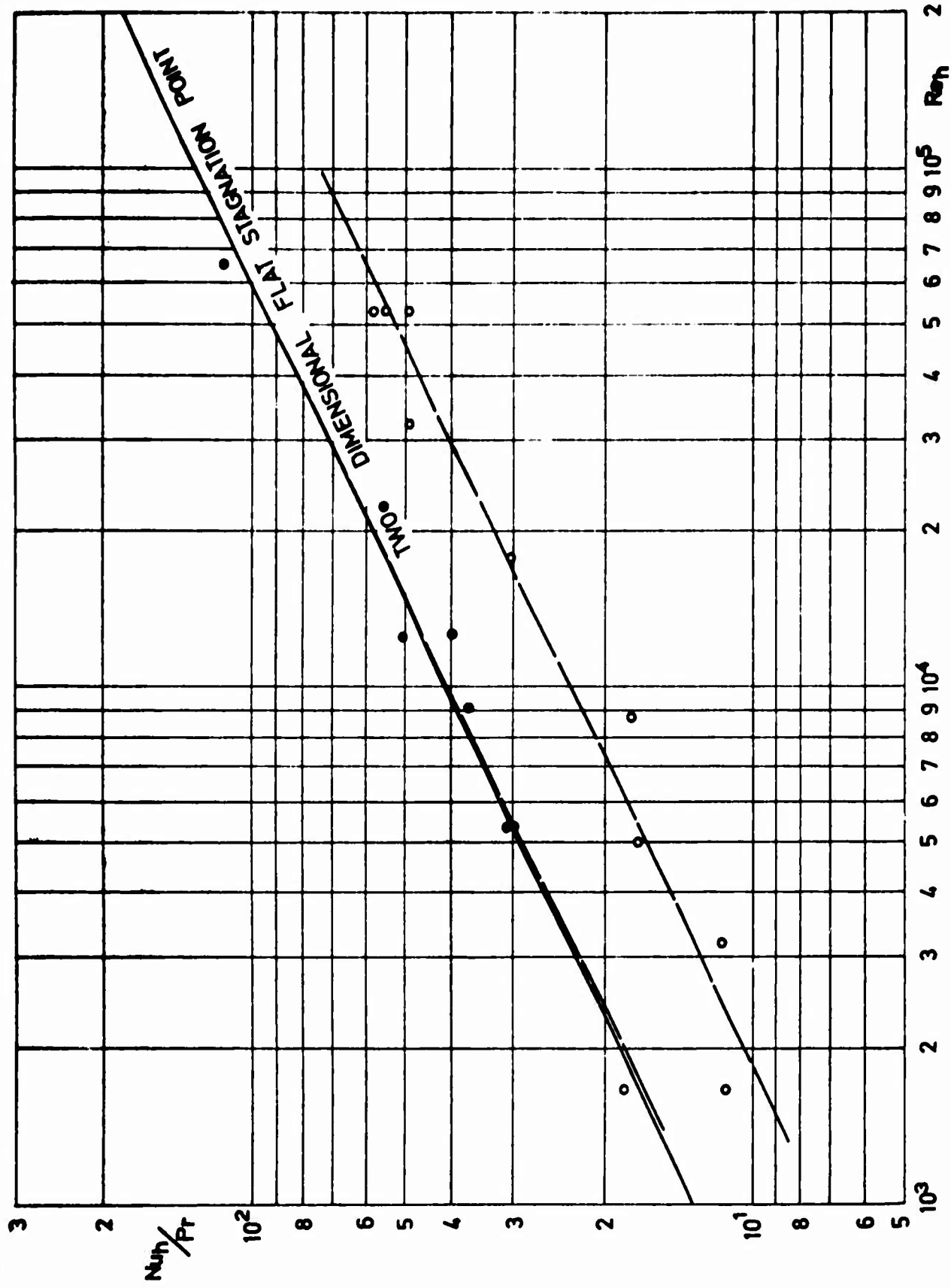


FIG. 6 (CONT.)

c) GAGE NO. 9 AT $x/h = 0.444$

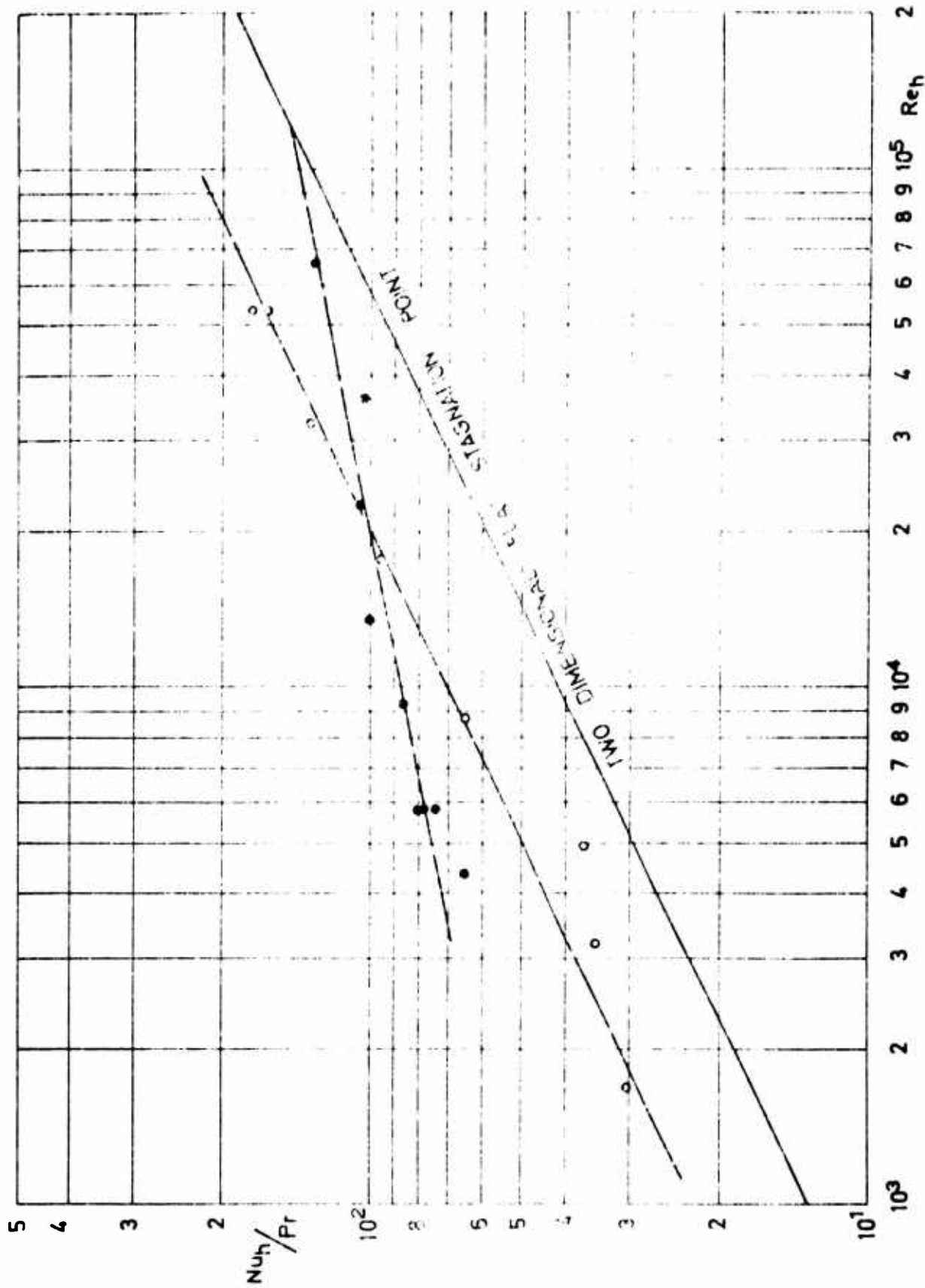


FIG. 6 (CONCL'D) d) GAGE NO. 10 AT $x/h = 0.836$

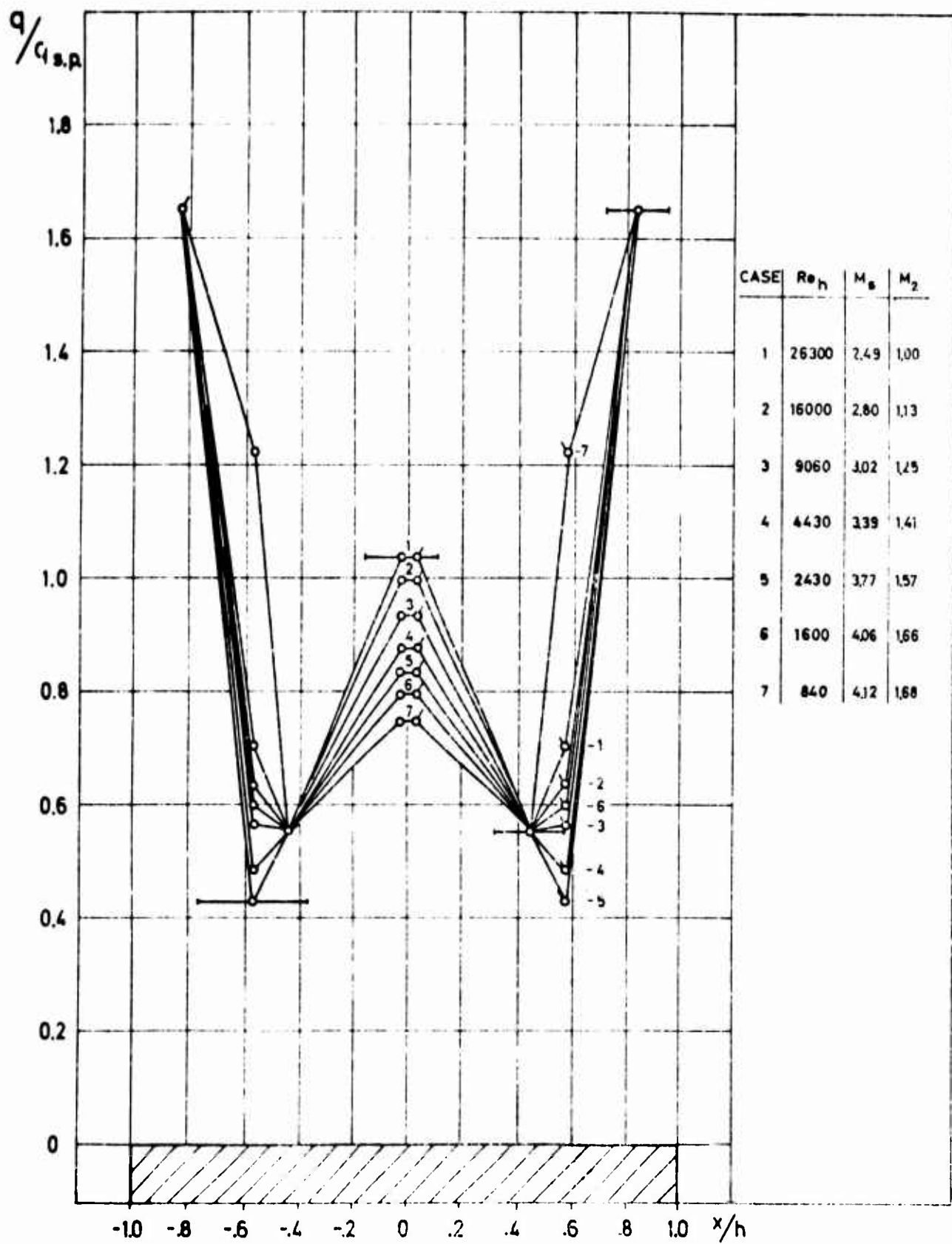


FIG. 7 HEAT TRANSFER VARIATION ON THE BLUNT FLAT NOSE

a) CHOKED FLOW -- AIR DRIVER GAS

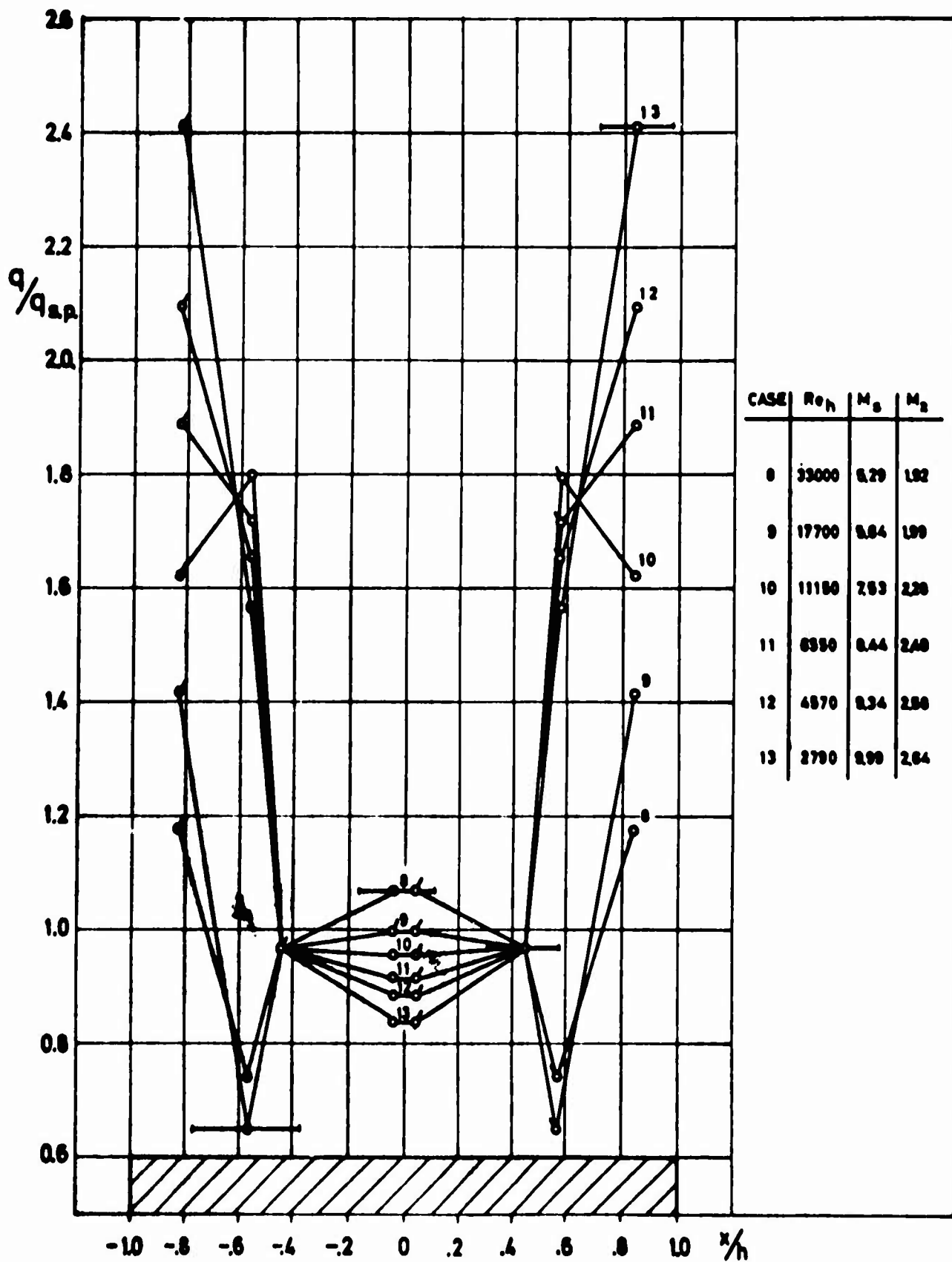


FIG. 7 (CONT.)

b) SUPERSONIC FLOW - HYDROGEN DRIVER GAS

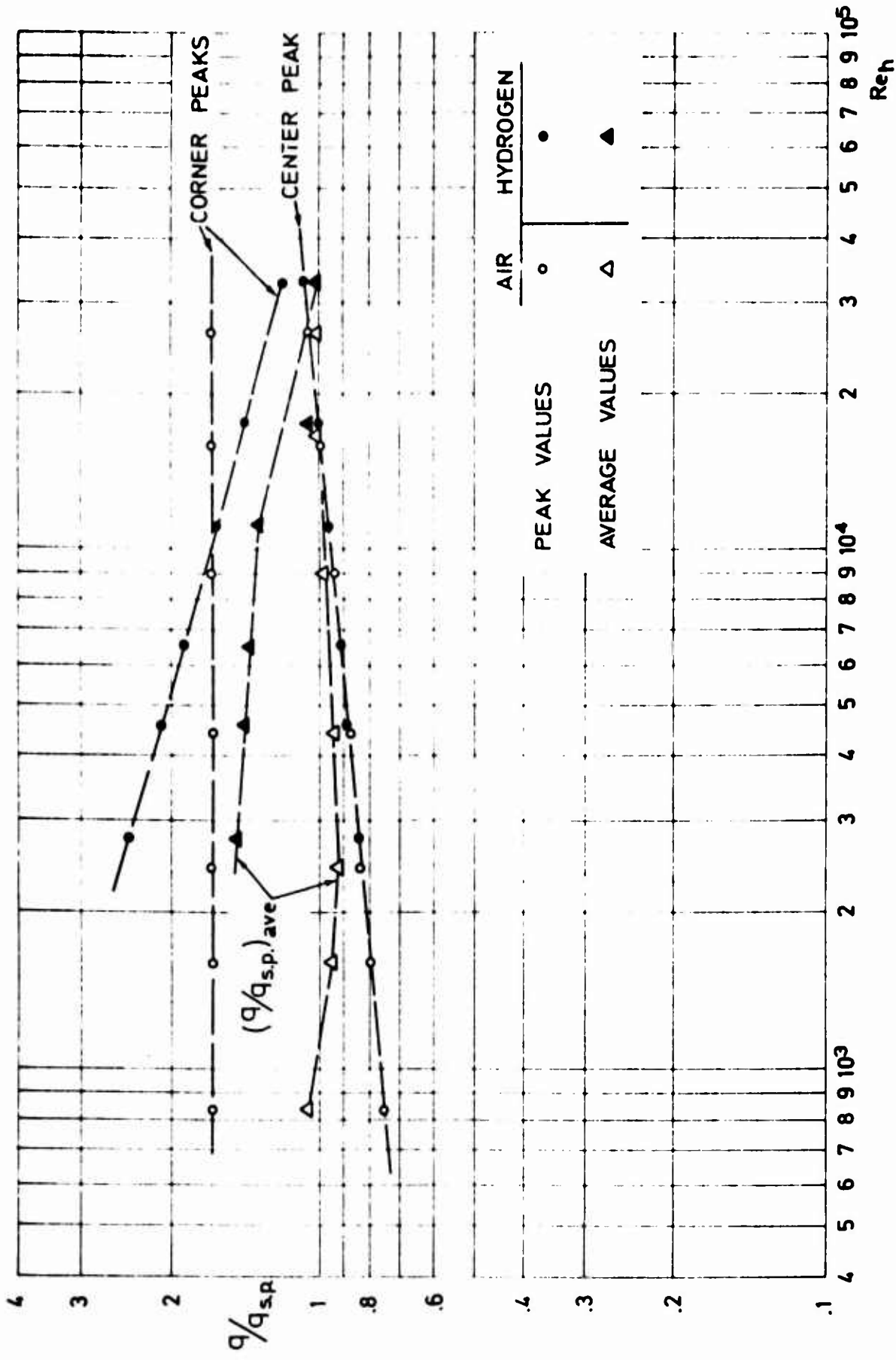


FIG. 7 (CONT.) c) MAXIMUM AND AVERAGE HEAT TRANSFER RATES ON THE FLAT NOSE

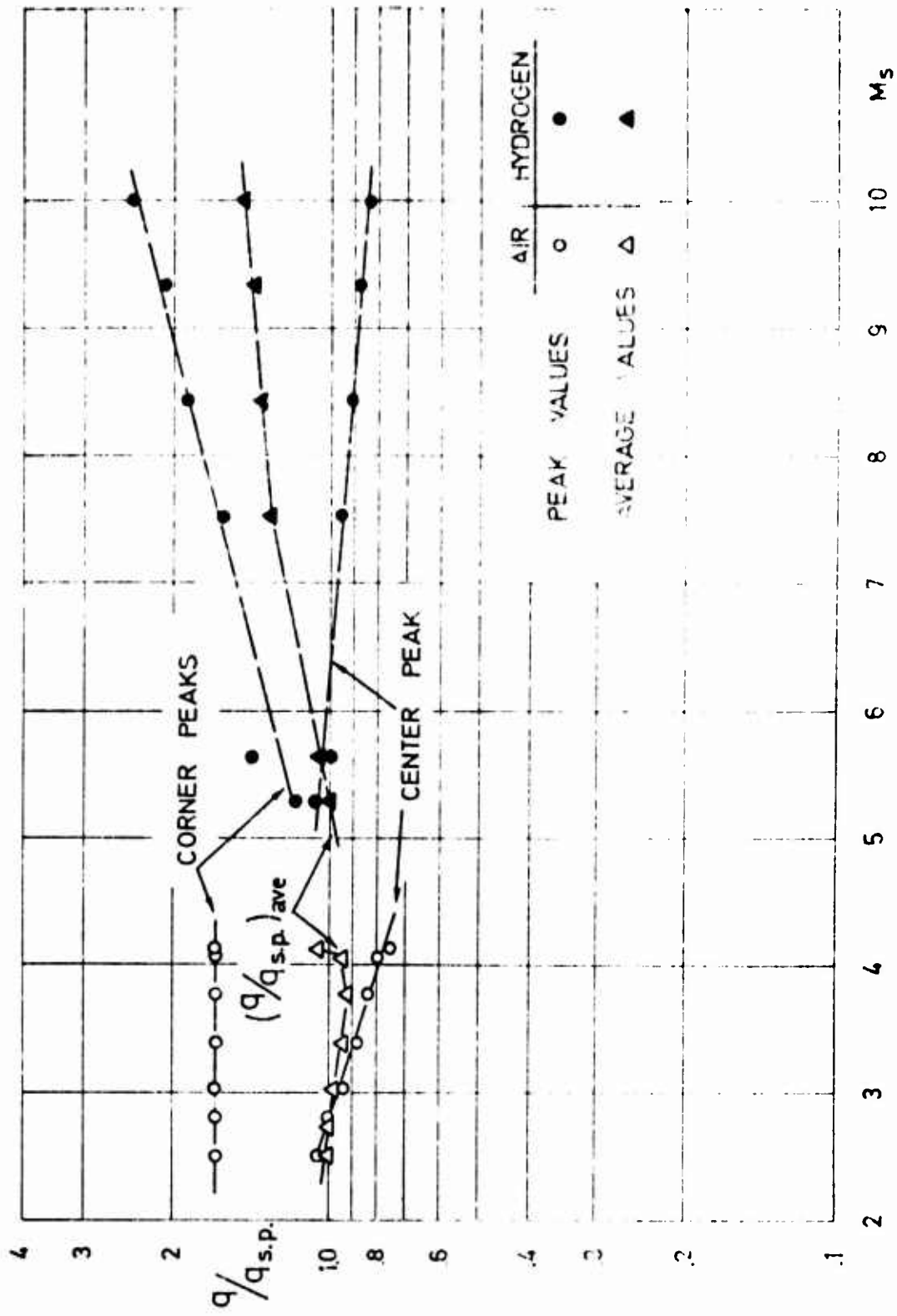


FIG. 7 (CONCL'D)

d) MAXIMUM AND AVERAGE HEAT TRANSFER RATES ON THE FLAT NOSE

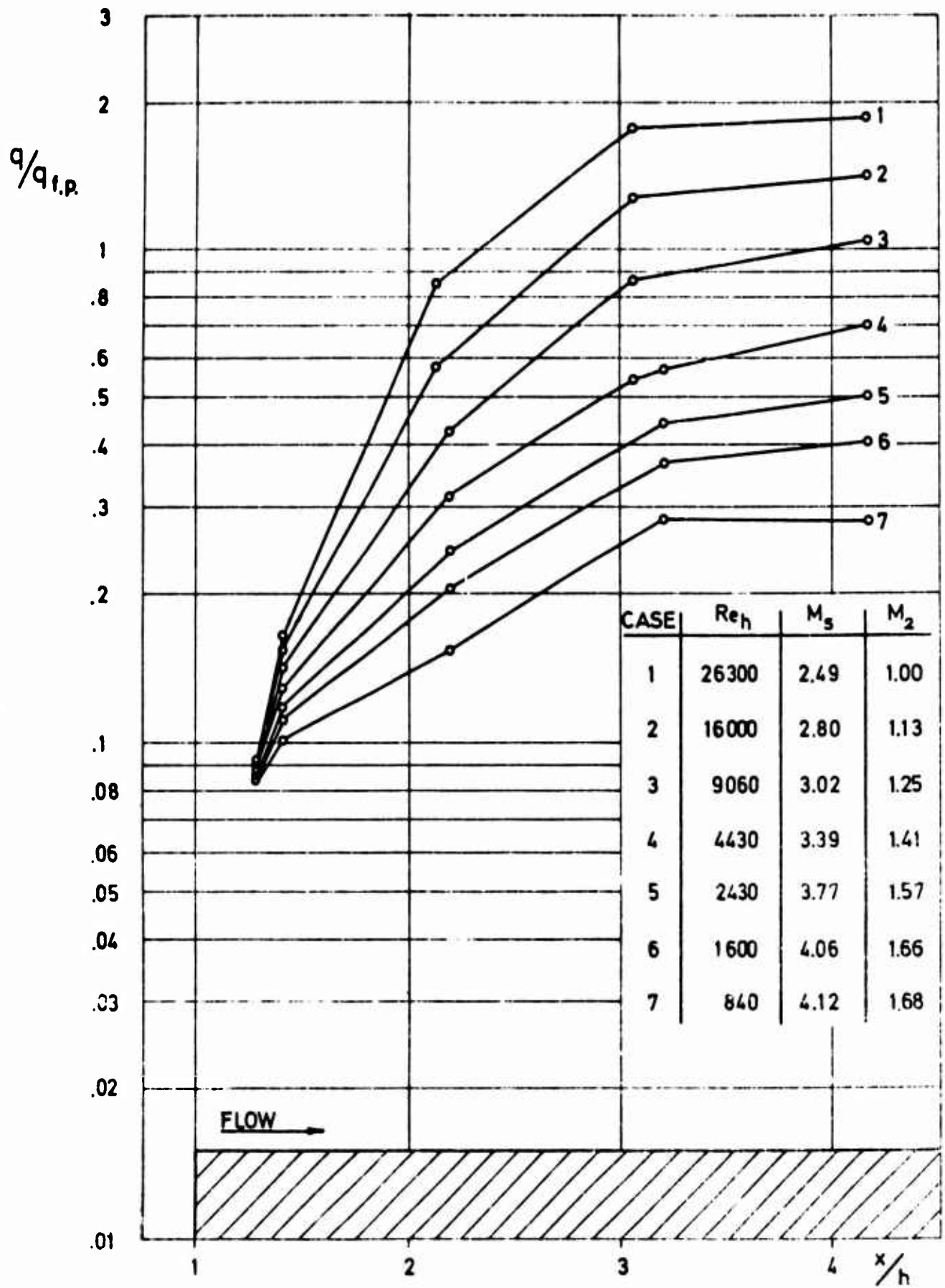


FIG. 2 HEAT TRANSFER RATE VARIATION BEHIND CORNER SEPARATION
 a) CHOKED FLOW - AIR DRIVER GAS

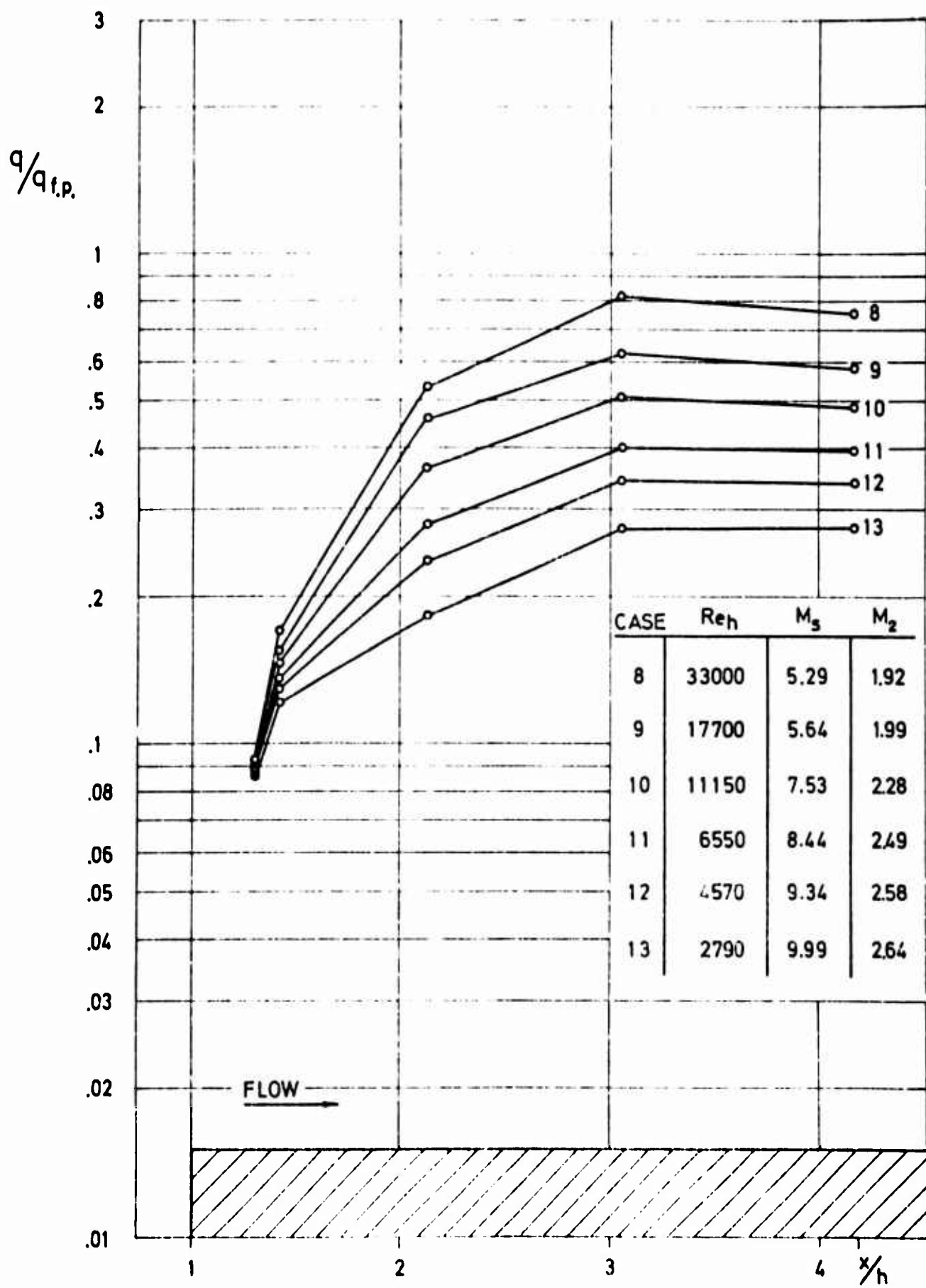


FIG. 8 (CONT.) b) SUPERSONIC FLOW -- HYDROGEN DRIVER GAS

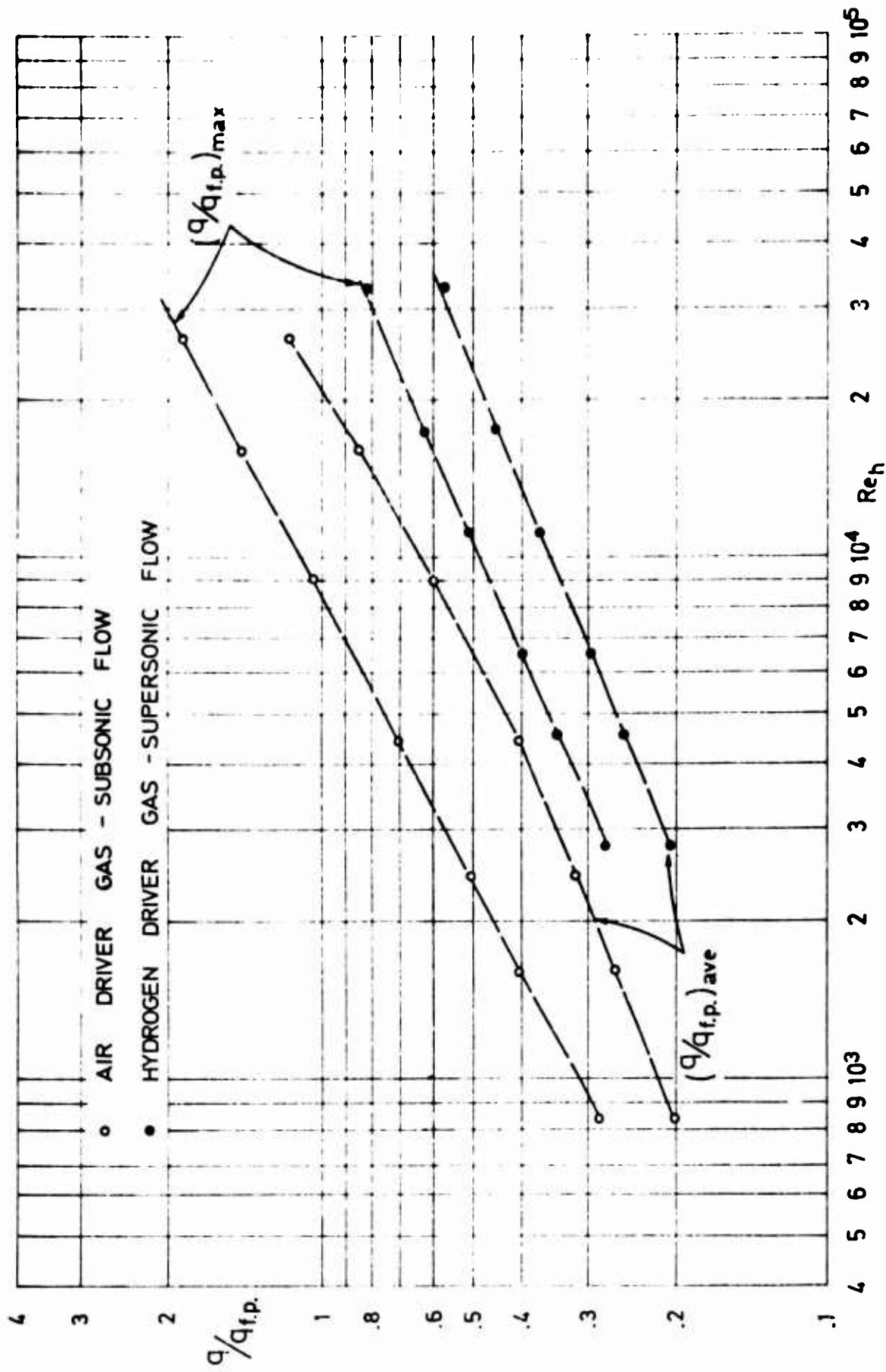


FIG. 8 (CONT.) c) MAXIMUM AND AVERAGE HEAT TRANSFER RATES AT LEADING EDGE SEPARATION BUBBLE

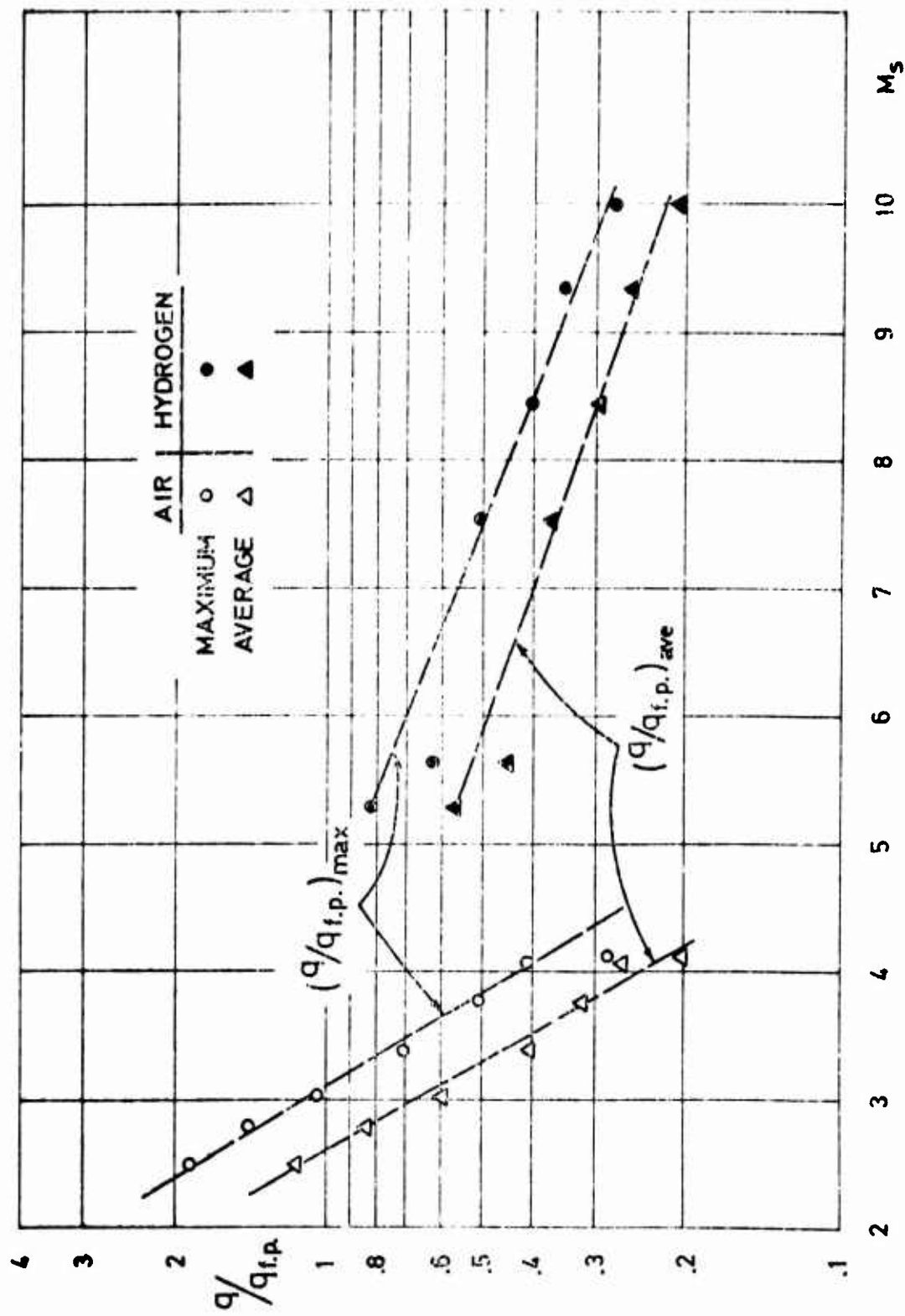


FIG. 8 (CONCL'D) d) MAXIMUM AND AVERAGE HEAT TRANSFER AT LEADING EDGE SEPARATION BUBBLE

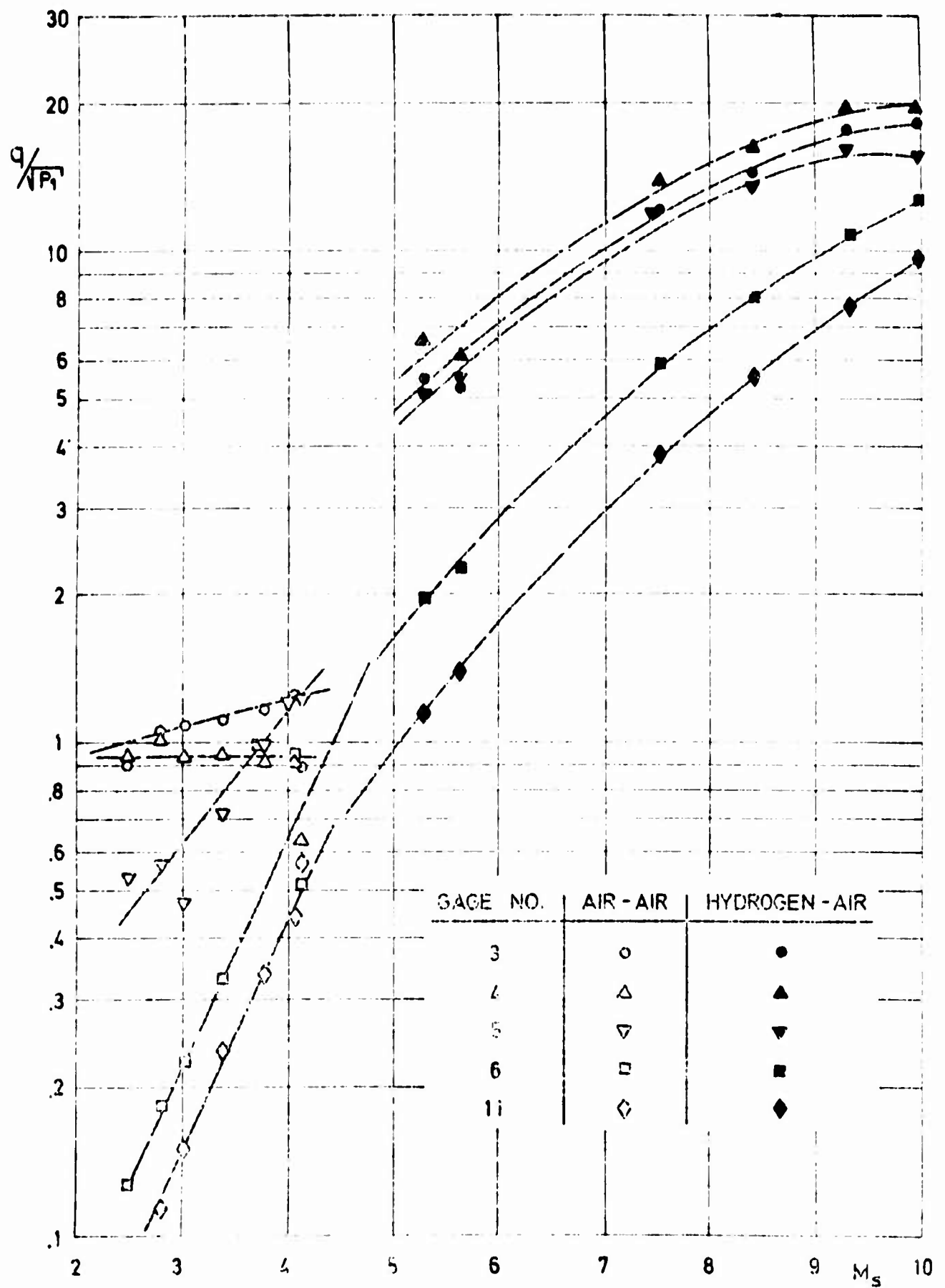


FIG 9

HEAT TRANSFER RATE VS. SHOCK MACH NUMBER

a) FLAT PLATE SECTION - SEPARATION BUBBLE DISTRIBUTION

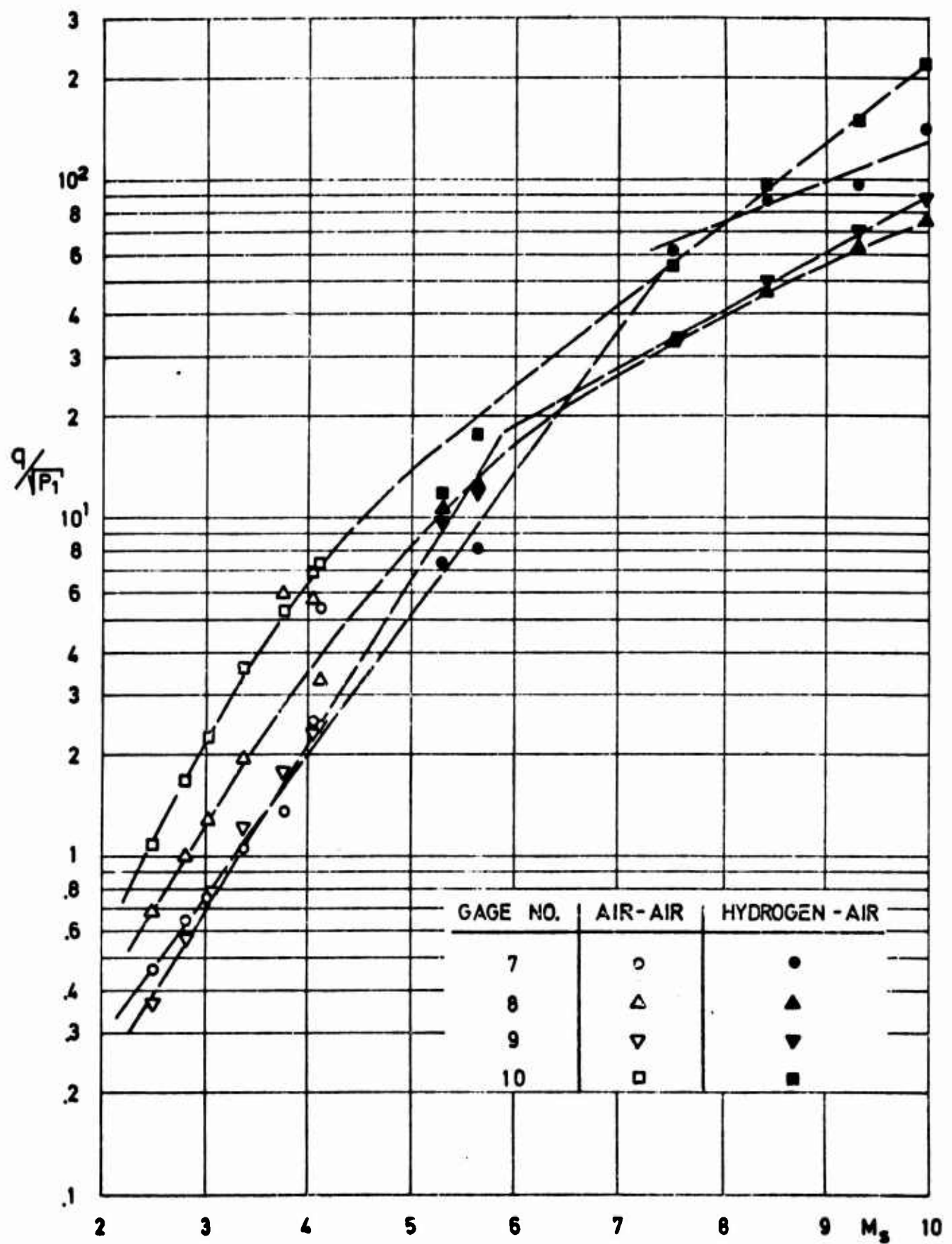


FIG. 9 (CONCL'D)

b) FLAT NOSE

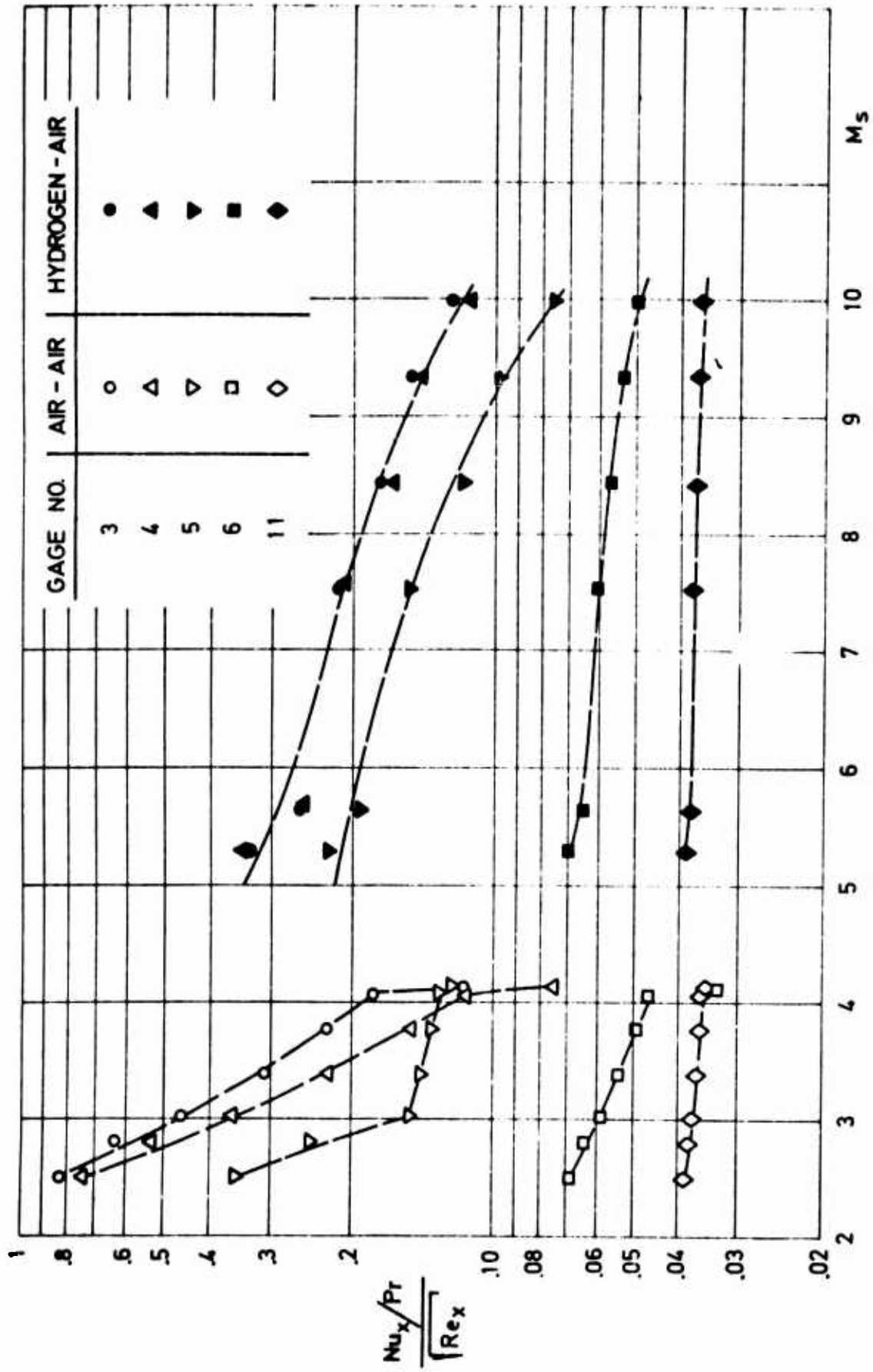


FIG. 10 $Nu_x / Pr \cdot Re_x^{1/2}$ VS. SHOCK MACH NUMBER

a) FLAT PLATE SECTION - SEPARATION BUBBLE

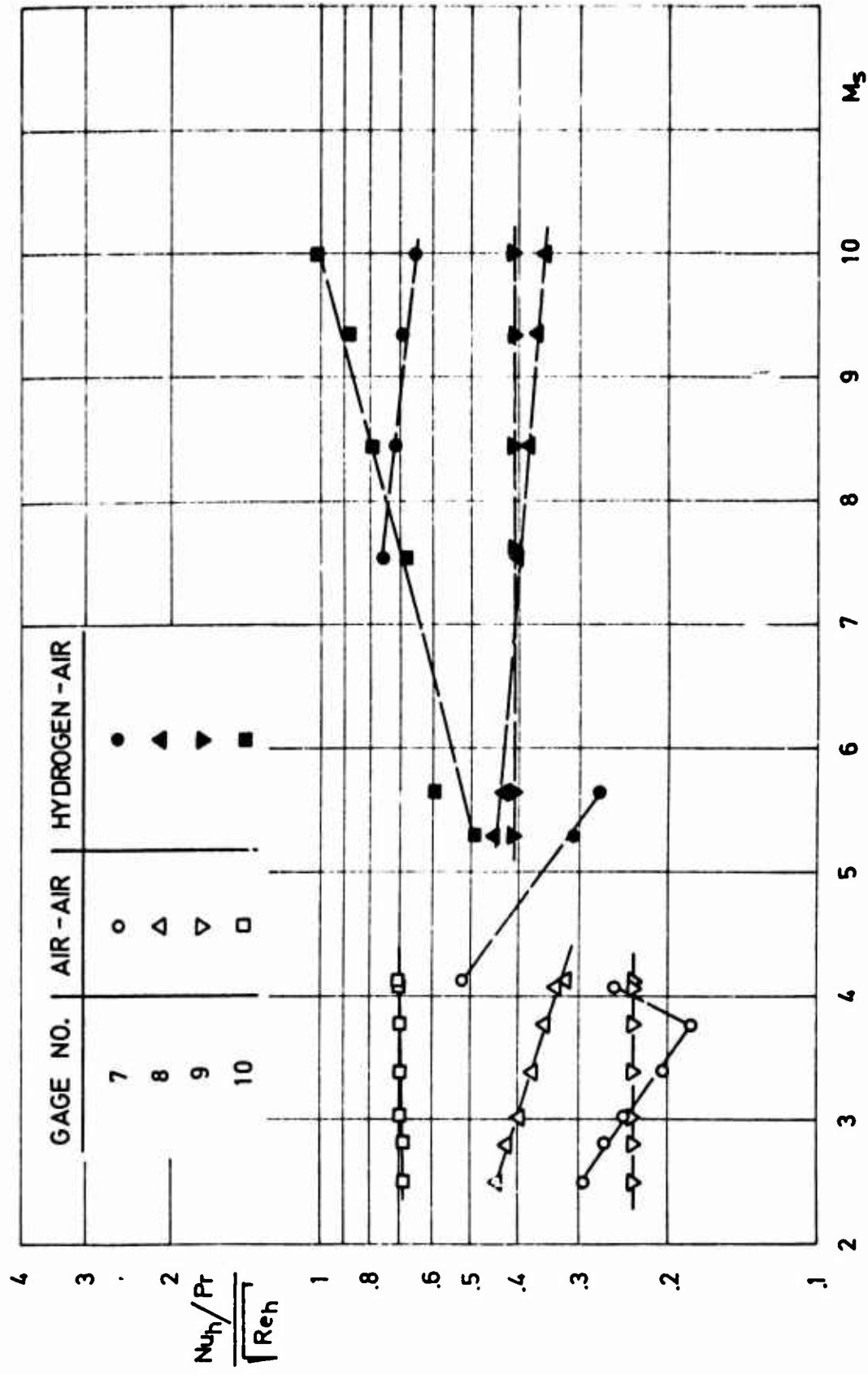


FIG. 10 (CONCL'D) b) ON THE FLAT NOSE

UNCLASSIFIED
Security Classification

DOCUMENT CONTROL DATA - R&D		
<i>(Security classification of title, body of abstract and indexing annotation must be entered when the overall report is classified)</i>		
1 ORIGINATING ACTIVITY (Corporate author) TECHNION RESEARCH AND DEVELOPMENT FOUNDATION AERONAUTICAL ENGINEERING LABORATORY, HAIFA, ISRAEL.		2a REPORT SECURITY CLASSIFICATION Unclassified
		2b GROUP
3 REPORT TITLE LAMINAR HEAT TRANSFER TO A TWO DIMENSIONAL BLUNT FLAT NOSED BODY IN TRANSONIC AND SUPERSONIC FLOW		
4 DESCRIPTIVE NOTES (Type of report and inclusive dates) Scientific Interim. Report No. 3		
5 AUTHOR(S) (Last name, first name, initial) Josef Rom Arnan Seginer		
6 REPORT DATE September 1967	7a TOTAL NO OF PAGES 43	7b NO OF REFS 12
8a CONTRACT OR GRANT NO. F61052 67 C 0033	9a ORIGINATOR'S REPORT NUMBER(S) TAE REPORT No. 75	
a PROJECT NO 7063		
c 61445014		
d 681307	9b OTHER REPORT NO(S) (Any other numbers that may be assigned this report)	
10 AVAILABILITY/LIMITATION NOTICES This document has been approved for public release and sale; its distribution is unlimited.		
11 SUPPLEMENTARY NOTES TECH, OTHER.	12 SPONSORING MILITARY ACTIVITY Aerospace Research Laboratories (ARN) Wright-Patterson AFB, Ohio 45433	
13 ABSTRACT <p>Heat transfer rates are measured on a two-dimensional, blunt, flat nose and in the separated and reattaching flow regions of the separation bubble behind the leading edge corners in the high enthalpy laminar transonic and supersonic flow in the shock tube.</p> <p>The measurements are carried out in a shock Mach number range from 2.5 to 10, and a corresponding flow Mach number from approximately 0.4 (the flow being choked) to 2.7. The Reynolds number, which is based on half of the nose height, varies from 8×10^2 to 3.3×10^4 and the local Reynolds number on the flat plate section, behind the leading edge corners, based on the distance from the stagnation point varies from 1×10^3 to 1.5×10^5.</p> <p>The results are correlated in terms of: (Nu/Pr), $(q/\sqrt{P_1})$ and $(Nu/PrRe^{1/2})$ as functions of Mach and Reynolds numbers and stagnation to wall enthalpy ratios. The variations of local maximum and average heat transfer rates on the nose section and in the separation bubble region behind the corner are presented.</p>		

DD FORM 1473
1 JAN 64

UNCLASSIFIED
Security Classification

UNCLASSIFIED

Security Classification

14 KEY WORDS	LINK A		LINK B		LINK C	
	ROLE	WT	ROLE	WT	ROLE	WT
1. Stagnation point heat transfer						
2. Blunt flat nose heat transfer						
3. Heat transfer in separated flow						
4. Supersonic separated flow						
5. Subsonic separated flow						
6. Supersonic stagnation point flow						
7. Subsonic stagnation point flow						
8. Laminar separated flow						

INSTRUCTIONS

1. **ORIGINATING ACTIVITY:** Enter the name and address of the contractor, subcontractor, grantee, Department of Defense activity or other organization (*corporate author*) issuing the report.
- 2a. **REPORT SECURITY CLASSIFICATION:** Enter the overall security classification of the report. Indicate whether "Restricted Data" is included. Marking is to be in accordance with appropriate security regulations.
- 2b. **GROUP:** Automatic downgrading is specified in DoD Directive 5200.10 and Armed Forces Industrial Manual. Enter the group number. Also, when applicable, show that optional markings have been used for Group 3 and Group 4 as authorized.
3. **REPORT TITLE:** Enter the complete report title in all capital letters. Titles in all cases should be unclassified. If a meaningful title cannot be selected without classification, show title classification in all capitals in parenthesis immediately following the title.
4. **DESCRIPTIVE NOTES:** If appropriate, enter the type of report, e.g., interim, progress, summary, annual, or final. Give the inclusive dates when a specific reporting period is covered.
5. **AUTHOR(S):** Enter the name(s) of author(s) as shown on or in the report. Enter last name, first name, middle initial. If military, show rank and branch of service. The name of the principal author is an absolute minimum requirement.
6. **REPORT DATE:** Enter the date of the report as day, month, year, or month, year. If more than one date appears on the report, use date of publication.
- 7a. **TOTAL NUMBER OF PAGES:** The total page count should follow normal pagination procedures, i.e., enter the number of pages containing information.
- 7b. **NUMBER OF REFERENCES:** Enter the total number of references cited in the report.
- 8a. **CONTRACT OR GRANT NUMBER:** If appropriate, enter the applicable number of the contract or grant under which the report was written.
- 8b, 8c, & 8d. **PROJECT NUMBER:** Enter the appropriate military department identification, such as project number, subproject number, system numbers, task number, etc.
- 9a. **ORIGINATOR'S REPORT NUMBER(S):** Enter the official report number by which the document will be identified and controlled by the originating activity. This number must be unique to this report.
- 9b. **OTHER REPORT NUMBER(S):** If the report has been assigned any other report numbers (*either by the originator or by the sponsor*), also enter this number(s).
10. **AVAILABILITY/LIMITATION NOTICES:** Enter any limitations on further dissemination of the report, other than those

imposed by security classification, using standard statements such as:

- (1) "Qualified requesters may obtain copies of this report from DDC."
- (2) "Foreign announcement and dissemination of this report by DDC is not authorized."
- (3) "U. S. Government agencies may obtain copies of this report directly from DDC. Other qualified DDC users shall request through _____."
- (4) "U. S. military agencies may obtain copies of this report directly from DDC. Other qualified users shall request through _____."
- (5) "All distribution of this report is controlled. Qualified DDC users shall request through _____."

If the report has been furnished to the Office of Technical Services, Department of Commerce, for sale to the public, indicate this fact and enter the price, if known.

11. **SUPPLEMENTARY NOTES:** Use for additional explanatory notes.
12. **SPONSORING MILITARY ACTIVITY:** Enter the name of the departmental project office or laboratory sponsoring (*paying for*) the research and development. Include address.
13. **ABSTRACT:** Enter an abstract giving a brief and factual summary of the document indicative of the report, even though it may also appear elsewhere in the body of the technical report. If additional space is required, a continuation sheet shall be attached.

It is highly desirable that the abstract of classified reports be unclassified. Each paragraph of the abstract shall end with an indication of the military security classification of the information in the paragraph, represented as (TS), (S), (C), or (U).

There is no limitation on the length of the abstract. However, the suggested length is from 150 to 225 words.

14. **KEY WORDS:** Key words are technically meaningful terms or short phrases that characterize a report and may be used as index entries for cataloging the report. Key words must be selected so that no security classification is required. Identifiers, such as equipment model designation, trade name, military project code name, geographic location, may be used as key words but will be followed by an indication of technical context. The assignment of links, rules, and weights is optional.

UNCLASSIFIED

Security Classification